GEOLOGICA CARPATHICA, DECEMBER 2013, 64, 6, 437–460 doi: 10.2478/geoca-2013-0030

An account of the bio- and magnetostratigraphy of the Upper Tithonian–Lower Berriasian interval at Le Chouet, Drôme (SE France)

WILLIAM A.P. WIMBLEDON[1], DANIELA REHÁKOVÁ[2], ANDRZEJ PSZCZÓŁKOWSKI[3], CRISTINA E. CASELLATO[4], EVA HALÁSOVÁ[2], CAMILLE FRAU[5], LUC G. BULOT[6], JACEK GRABOWSKI[7], KATARZYNA SOBIEŃ[7], PETR PRUNER[8], PETR SCHNABL[8] and KRISTÝNA ČÍŽKOVÁ[8]

[1]Department of Earth Sciences, University of Bristol, Queens Road, Bristol BS8 1RJ, United Kingdom; mishenka1@yahoo.co.uk; glwapw@bristol.ac.uk
[2]Department of Geology and Paleontology, Faculty of Natural Sciences, Comenius University, Mlynská dolina G-1, 842 15 Bratislava, Slovak Republic; rehakova@fns.uniba.sk; halasova@fns.uniba.sk
[3]Institute of Geological Sciences, Polish Academy of Sciences, ul. Twarda 51/55, PL-00-818 Warsaw, Poland; pszczolkowski@yahoo.com
[4]Dipartimento di Scienze della Terra "A. Desio", Università degli Studi di Milano, via Mangiagalli 34, 20133 Milano, Italia; cristina.casellato@unimi.it
[5]Biogéosciences, UMR-CNRS 5561, Université de Bourgogne, 6 Bd Gabriel, 21000 Dijon, France; camille_frau@hotmail.fr
[6]Géologie de Système Carbonatés, Université de Provence Aix-Marseille, Case 57, 3 place Victor Hugo, F 13331 Marseille, France; lucgbulot@aol.com
[7]Polish Geological Institute–National Research Institute, Rakowiecka 4, 00-975 Warsaw, Poland; jacek.grabowski@pgi.gov.pl; katarzyna.sobien@pgi.gov.pl
[8]Institute of Geology AS CR, v.v.i., Rozvojová 269, 165 00 Praha 6, Czech Republic; pruner@gli.cas.cz; schnabl@gli.cas.cz; cizkovak@gli.cas.cz

(Manuscript received January 7, 2013; accepted in revised form October 16, 2013)

Abstract: This paper discusses the results of a study of the Le Chouet section, its lithologies, facies, magnetic properties and fossil record (ammonites, calcareous nannofossils, calpionellids and calcareous dinoflagellates). Data obtained have been applied to give a precise biostratigraphy for this carbonate sequence as well as a paleoenvironmental reconstruction. Its relationship to magnetostratigraphy, based on a modern study of a French site, is important. Investigation of the micro- and macrofossils shows that the site comprises a sedimentary sequence in the Microcanthum to Jacobi ammonite Zones, and the *Chitinoidella*, *Crassicollaria* and *Calpionella* Zones. Several calpionellid and nannofossil bioevents have been recorded on the basis of the distribution of stratigraphically important planktonic organisms. The site allows us to calibrate the levels of various biomarkers and biozonal boundaries, and correlate them with the magnetozones M20n, M19r and M19n.

Key words: Tithonian, Berriasian, integrated biostratigraphy, magnetostratigraphy, microfacies, ammonites, calcareous nannofossils, calcareous dinoflagellates, calpionellids.

Introduction

This study results from the decision of the Berriasian Working Group (International Subcommission on Cretaceous Stratigraphy) to better document sequences at and close to the Jurassic/Cretaceous (J/K) boundary, and it is our intention to publish comparative accounts of the best-developed sections, in line with the multidisciplinary standards exemplified by the studies made by Michalík et al. and Houša et al. Simultaneously, working-group members are re-examining classical localities and new sites to better assess and calibrate useful topmost Tithonian to lowest Berriasian markers and their proxies (Wimbledon et al. 2011). Significantly, though we commence work on the classical European sites, we are extending detailed study out from this core area to new sites in Africa, Asia and the Americas to better constrain the J/K boundary.

As at the historical stratotype of Berrias fossiliferous units do not extend low enough to reach the putative base for the Cretaceous, it is unsuitable for our purposes of stage and biozonal definition. Therefore, a start has been made on examining other localities in southern France — seeking 'templates' for the top Tithonian ("*Durangites* Zone"), and the *Berriasella jacobi* and *Pseudosubplanites grandis* zonal intervals. These included the only locality that had been noted with a relatively common latest Tithonian ammonite assemblage (Boughdiri 1994), and that is the section described in this work. A first reconnaissance in 2008 located the site, but also revealed the existence of common ammonite faunas overlying the supposed *Durangites*-bearing levels, and therefore the section was chosen for closer study; and it was then additionally sampled for calpionellids, calcareous nannofossils and, subsequently, magnetostratigraphy. Further work at this productive site on geochemistry, magnetic susceptibility, refinement of results on magnetostratigraphy, calpionellids and ammonites is still in progress and this will form a basis for further publications.

This paper is the first description of the locality, in the Fournet Ravine, 10 km SE of Luc-en-Diois, Drôme; a site straddling the top Tithonian and lowest Berriasian stages. Locally, well-bedded and massively bedded (averaging 0.20–1.00 m) Berriasian limestones form the upper slopes of the steep valley sides. Massive breccias (Remane 1970) in the Tithonian and Berriasian, sometimes tens of metres in thickness, are a dominating element of the landscape, forming inaccessible cliffs in local valleys.

Regionally, the Le Chouet and nearby Drôme sections (see Fig. 1) are part of the succession of the Domain vocontien or Basin vocontien (the Fosse Vocontienne or Vocontian trough of many earlier publications). This depositional basin occupies an approximately triangular area, its base extending across Languedoc and Provence, 250 km west to east, with a prolongation northwards to a narrow apex which reaches as far as Lake Geneva. Sedimentation was confined by older basement massifs: in the west by the Cévennes (Massif Central) and Les Maures in the south, with an opening eastwards to the oceanic Tethys. In the Upper Jurassic to lowest Cretaceous transition, it contains a sequence of deeper-water pelagic and hemipelagic sediments, whereas in some areas there were marginal marine or even terrestrial Purbeck facies, including evaporites, notably in the north (Maillard 1884; Détraz & Mojon 1989, etc.).

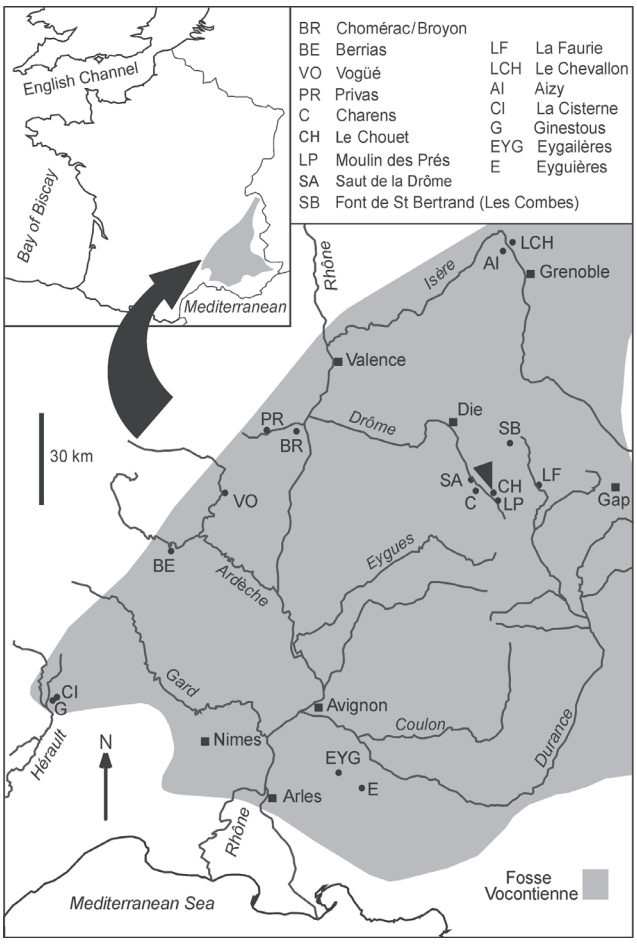

Fig. 1. Locality map of the Fosse Vocontienne, SE France.

The 'trough' thus includes classical areas and sites that have figured in studies of the Late Tithonian–Berriasian (Mazenot 1939; Le Hégarat 1971; Fig. 1 herein) — sites in the SW in the valley of the Hérault, along the River Ardèche (with the nominal type locality of Berrias), near Privas, including Chomérac, and across the catchments of the Durance, the Drôme and ultimately the River Isère, near to Grenoble. Putatively, the junction between the Tithonian and Berriasian in the western Tethys has been placed in ammonite schemes at the junction of the "*Durangites* Zone" and the *Berriasella jacobi* Subzone, despite the absence of any "*Durangites*" fauna. This has been the case among the classical French localities, many of which show abundant *Berriasella jacobi* assemblages, albeit often from breccia/conglomerate horizons, though very few have yielded any "*Durangites*".

Three previous authors have made significant mention of the Le Chouet site and its environs. Le Hégarat (1971) in his seminal work figured a somewhat stylized section for "Le Chouet" (as he did for other local sites). In that work he showed higher stratigraphic levels than are seen in the roadside section described here, and this seems to indicate another or a composite profile; perhaps involving outcrops further north, in the upper wooded reaches of the Fournet Valley (an area currently being studied). Remane (1970) gave an account of breccia developments in the Tithonian-Berriasian carbonates of the Drôme region, including both Le Chouet and the nearby Charens gorge section (3 km to the SSW). Remane's column for Le Chouet relates well to the section presented here: notably to eight useful marker beds up to his unit 1, breccias and conglomerates, which provide obvious comparable datums. Boughdiri (unpublished 1994) paid particular attention to the middle part of the sequence at Le Chouet, where he identified the *Durangites* Zone, illustrating several key ammonites, and noting a numbers of species of *Durangites* between our bed 78 and bed 85 (Fig. 11). Some of these ammonites were subsequently figured by Enay et al. (1998). Boughdiri also sampled seventeen levels for calpionellids, fixing the top of subzone A1 at the base of our bed 71 and the base of the *Calpionella* Zone at the base of bed 100.

Setting and geological description

In Late Jurassic to Late Cretaceous times, alternating periods of marl and limestone deposition characterized the region: however, in most areas during the Tithonian and the Berriasian, limestones were more common than marls: some few nearby Lower Berriasian sites have well-developed marl intervals (e.g. the sites of Saut de la Drôme and Les Combes (Fig. 1; Le Hégarat 1971)), but Le Chouet is more typical in comprising limestones.

The locality lies in the cliffed upper valley of the River Drôme, in pine forest (Long 5°33′33″ E, Lat 44°32′32″ N) off the local road (D306) from Die to Valdrôme. It comprises a low mural section, 200 m-long, along a single-track road on the north-west side of a precipitous gorge, the Ravin de Fournet. The section extends around the slope from an altitude of 928 m to a little above 1000 m. The sequence dips 10 degrees

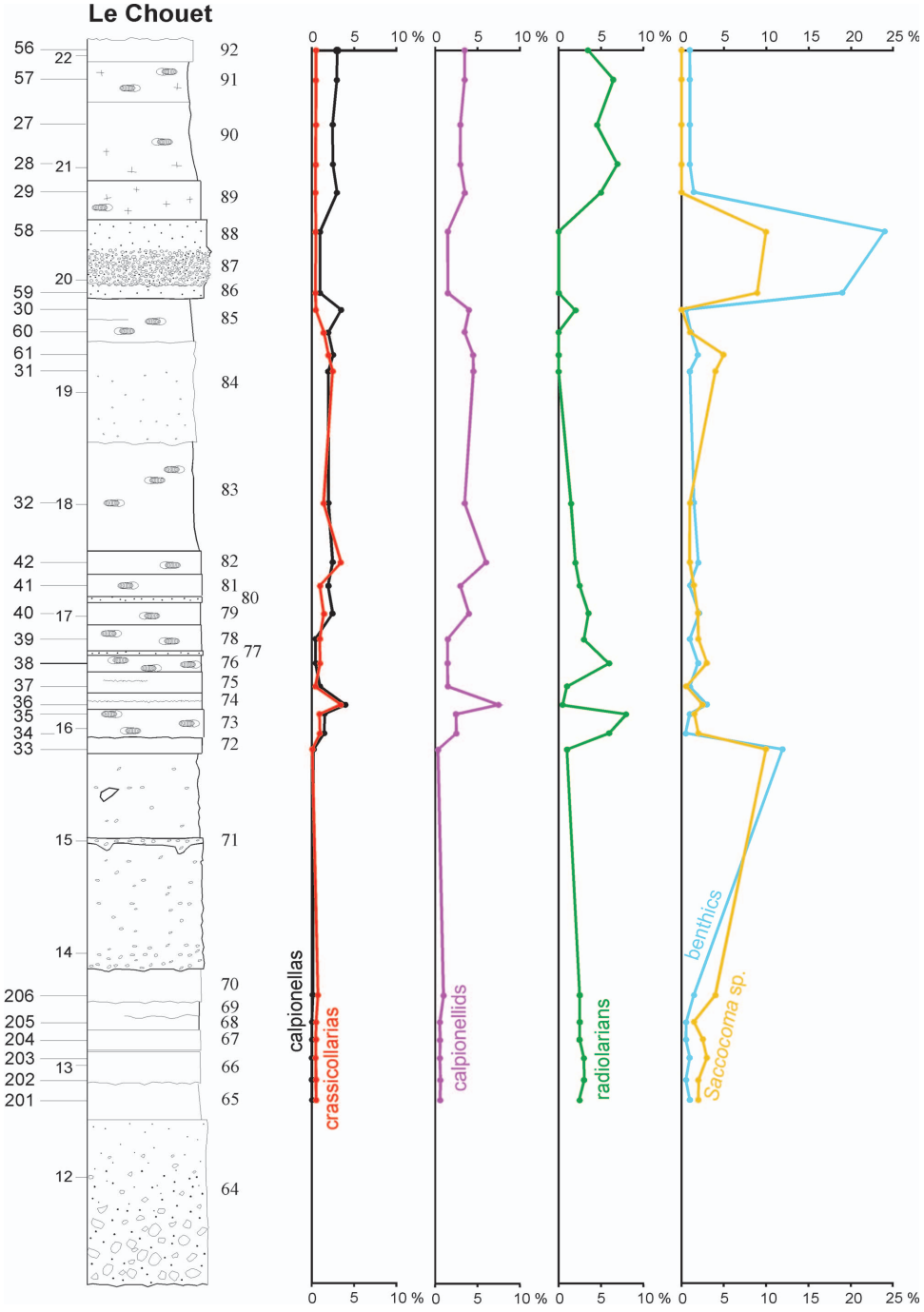

Fig. 2. Micropaleontological analysis — quantification of calpionellids and accompanying microfossils *sensu* Bacelle & Bossellini (1965).

at 155. The name for this trackside section previously used in the geological literature is that of the hamlet of Le Chouet (Le Chuot on older maps), which lies about 400 metres to the west of the section. Outcrops at supposed higher stratigraphic levels along the road to Le Chouet are not in stratigraphic continuity with the sequence here described, and tectonic dislocations are apparent between the broken exposures.

The succession exposed totals 43 metres, which includes, topping the section, a 10 m-thick, partly obscured, massive or poorly bedded micrite (bed 123) with 'floating' pebbles (Fig. 11). The majority of it consists of well-bedded micrite and biomicrite — mudstone, wackestone and packstone. Massive conglomerates and breccias (both clast and matrix supported) punctuate the sequence, and a number of intraclastic/microbreccia beds (grainstones) (e.g. beds 80, 108, 111; Fig. 11), grey in colour, alternate with the monotonous micrites. Pebble, boulder and grainstone levels make useful marker beds. These are variable in their grain sizes and textures, as noted in this region by Remane: units with coarse bases (e.g. beds 64, 71), 'floating' larger clasts in micrite (e.g. beds 71, 84, 104, 131), clast-supported beds (bed 87), and graded bedding (e.g. beds 52, 57, 64). Some of the thicker coarse-grained units mentioned above may be relatable to NW-SE submarine paleo-canyons that have been mapped in this region by Beaudoin and others (e.g. Joseph et al. 1988). Both Le Chouet and Charens lie inside one of the major canyons thus described, the Canyon de Ceuse. A range of slope and basinal settings have been postulated for Lower Berriasian sediments in the region, and origins as slumps, fans and channel fills have been suggested (e.g. Jan du Chęne et al. 1993). Only the lower beds (7–8 m) (not discussed in detail in this account) here show any appreciable argillaceous partings or thin beds, and therefore detectable indications of sedimentary rhythmicity.

Body fossils, apart from ammonites and aptychi, are rare; occasional isolated bivalves occur (common in a few beds), pygopid brachiopods have been noted, and common belemnites are found at one level (bed 103). Ammonites are numerous, excepting in the lowest ten metres, and most common in the central part of the sequence. Derived, abraded ammonites have been recorded in beds 64, 71, 87 and 123.

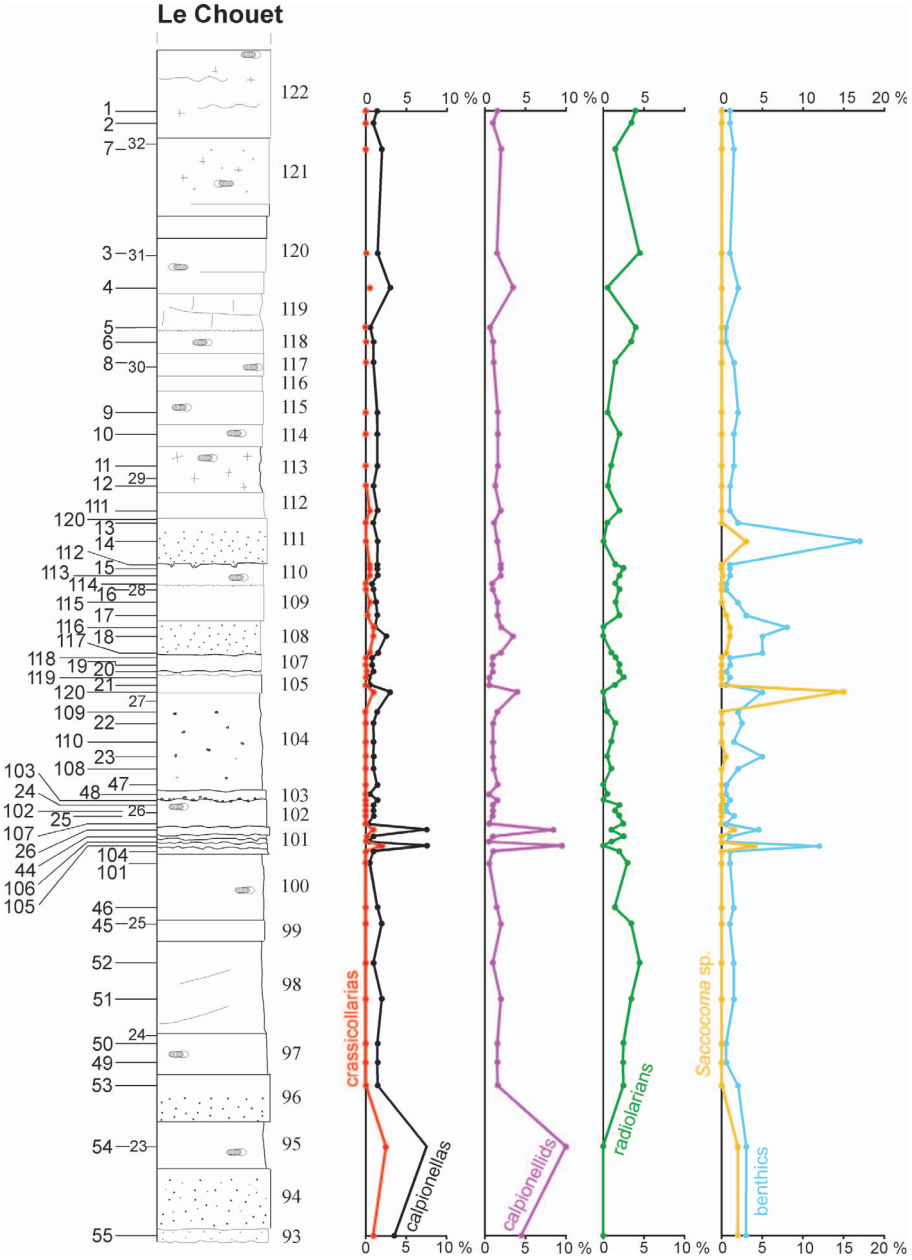

Fig. 3. Micropaleontological analysis — quantification of calpionellids and accompanying microfossils *sensu* Bacelle & Bossellini (1965).

Calpionellids and calcareous dinoflagellates — microfacies analysis

Samples used for microfacies analysis were collected in several steps; an initial 60 samples were later augmented at critical levels, to a total of 85 samples from an interval of 20 metres, between bed 65 and bed 122. (Higher and lower stratigraphic levels have since been sampled and these are currently being evaluated.) Allochems and micrite have been studied under an optical microscope (LEICA DM 2500) and the percentage rations of organic detrital grains, bioclasts etc. calculated. The data obtained are shown in graphic form, a representation of their relative changes (Figs. 2 and 3). Microfossil markers and microfacies were documented using a LEICA DFC 290 HD camera. The thin sections are stored in the collections of the Department of Geology and Paleontology (Faculty of Natural Sciences) in Bratislava.

The sequence studied is composed of biomicrite limestones (mudstones to wackestones) intercalated with pelbiomicrite, pelbiomicrosparite (packstones) and biomicrobrecciated limestones (grainstones). Calpionellids, radiolarians, saccocomids and residual biodetrital fragments have been quantitatively evaluated using the optical charts of Bacelle & Bosellini (1965). Intraclast fragments and saccocomids, crinoids, pellets and ooids were transported and resedimented, influenced probably by extensional pulses, synsedimentary erosion and/or eustatic fluctuations. Some intercalations bear the marks of storm sedimentation. Calpionellid and radiolarian curves are plotted on graphs (Figs. 2, 3), and they show a decrease in the abundance of calcareous plankton correlated with an increase of silica-producing organisms, as previously documented (Reháková & Michalík 1994; Michalík et al. 2009).

Calpionellids in the studied samples are generally well-preserved. Hyaline forms dominate. The calpionellid biostratigraphical scale (standard calpionellid zones and subzones) as proposed by Remane et al. (1986) and Reháková & Michalík (1997) and the calcareous dinoflagellate succession *sensu* Reháková (2000) have been adopted. Two calpionellid zones are well recognized, the *Crassicollaria* Zone (with Remanei, Intermedia and Colomi Subzones) and the *Calpionella* Zone (Alpina Subzone) (Fig. 4), with a less defined *Chitinoidella* Zone (Boneti Subzone) below.

Chitinoidella Zone, Boneti Subzone (*sensu* Borza 1984 and Grandesso 1977)

This zone has been identified on the basis of a few, spaced, samples. In beds below the thick mass-flow unit of bed 64, calpionellids are less common. The lowest 5 m of the

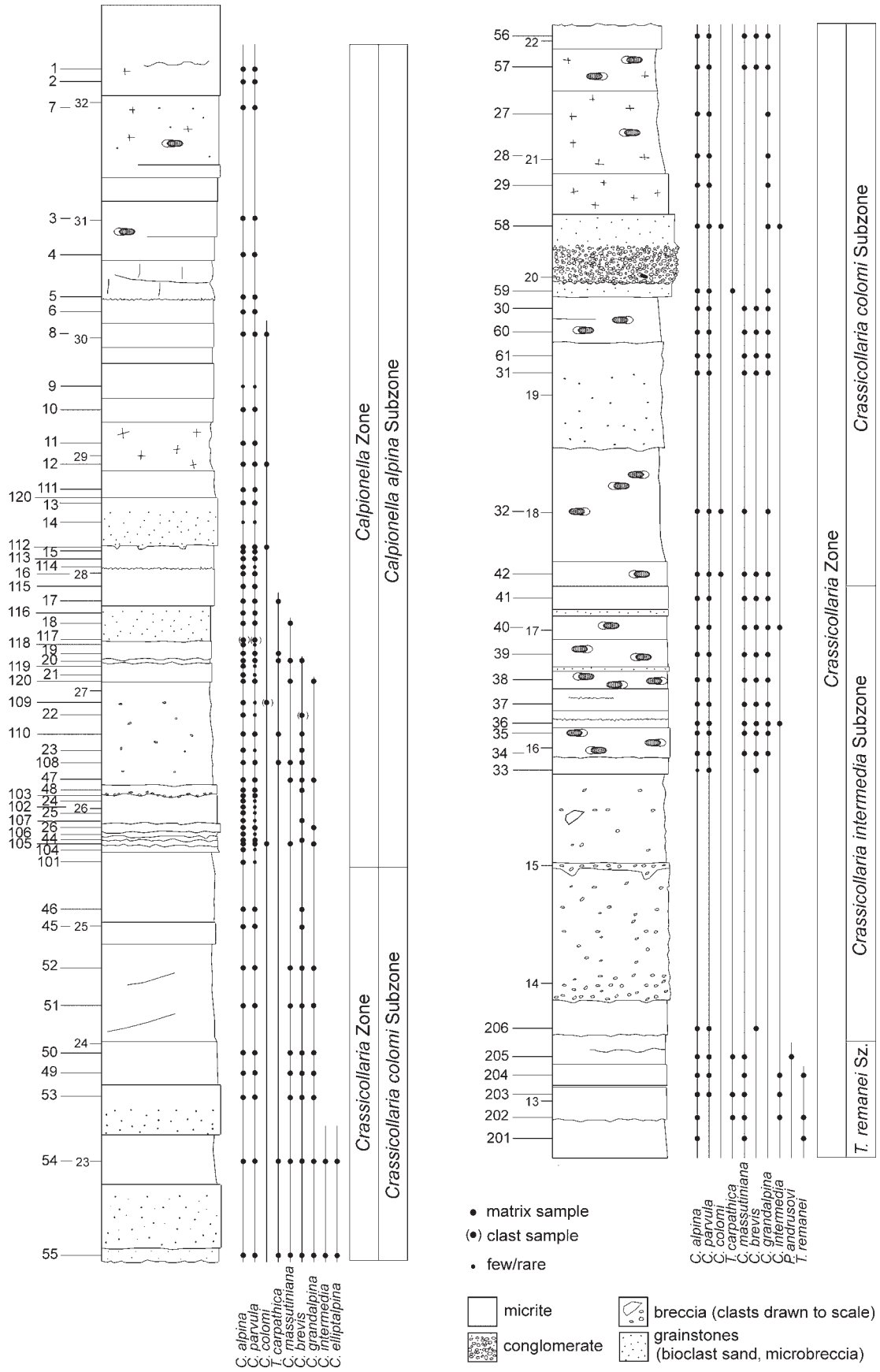

Fig. 4. Vertical ranges of calpionellid species. (Lithologies shown apply to all figures.)

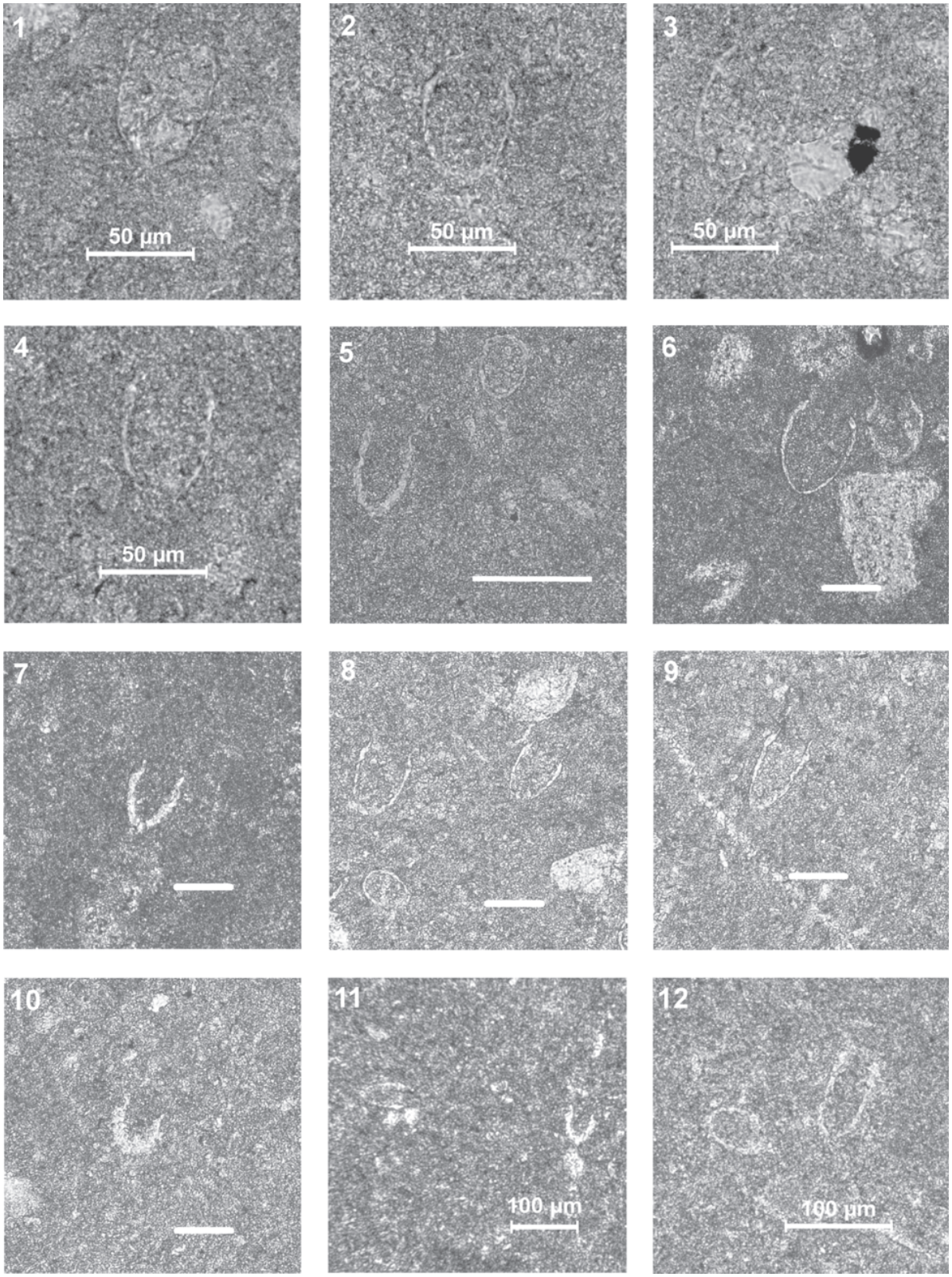

Fig. 5. 1 — *Praetintinnopsella andrusovi* Borza; Sample CH205. **2** — *Tintinnopsella remanei* Borza; Sample CH204. **3** — *Tintinnopsella carpathica* (Murgeanu & Filipescu); Sample CH203. **4** — *Crassicollaria massutiniana* (Colom); Sample CH206. **5** — *Crassicollaria* aff. *intermedia* (Durand Delga); Sample CH61. **6** — *Calpionella elliptalpina* Nagy; Sample CH55. **7** — *Crassicollaria brevis* Remane; Sample CH55. **8** — *Crassicollaria massutiniana* (Colom), *Crassicollaria parvula* Remane; Sample CH47. **9** — *Crassicollaria parvula* Remane; Sample CH47. **10** — *Calpionella alpina* Lorenz; Sample CH47. **11** — *Crassicollaria brevis* Remane; Sample CH110. **12** — *Crassicollaria colomi* Doben; Sample CH109. Scale bars in Figs. 5–10 are 100 µm.

Le Chouet section have yet to be sampled for microfossils, but the next 5.5 m (beds 33 to 63), mostly consisting of biomicrites, yield rare benthic forams (*Spirillina*, beds 50 and 56), poorly preserved calcified radiolaria (mostly noticeably possible *Spumellaria*), *Saccocoma* ossicles, and a few levels with chitinoidellids. Calcareous dinoflagellates are practically absent from the interval. The majority of samples demonstrate radiolarian-*Saccocoma* microfacies and lesser radiolarian microfacies (13 of 19 samples), with a few occurrences of *Saccocoma* microfacies and one of radiolarian-*Saccocoma-Globochaete* microfacies.

Chitinoidellids are scarce below bed 64, but they have been identified in beds 33, 34 and 61, albeit with poor preservation. Bed 33 yields *Chitinoidella* cf. *boneti* Doben and *Carpathella rumanica*, bed 34 has *Longicollaria* cf. *dobeni*, and bed 59 *Chitinoidella* ex gr. *boneti-elongata* and indeterminate Chitinoidellidae. Their presence makes it possible to assign at least beds 33 to 59 to the *Chitinoidella* Zone.

Crassicollaria Zone, Remanei Subzone (*sensu* Remane et al. 1986) — samples CH201–CH205

Biomicrite limestones of globochaete-radiolarian microfacies (wackestones): they contain calcified radiolarians, sponges, globochaetes, ?*Praetintinnopsella andrusovi* Borza (Fig. 5.1), *Tintinnopsella remanei* Borza (Fig. 5.2), *Tintinnopsella carpathica* (Murgeanu & Filipescu), *Crassicollaria intermedia* (Durand Delga), *Crassicollaria massutiniana* (Colom), *Crassicollaria parvula* Remane, *Calpionella alpina* Lorenz, cysts of *Stomiosphaera moluccana* Wanner (Fig. 6.1), *Stomiosphaerina proxima* Řehánek, *Colomisphaera nagyi* (Borza) (Fig. 6.2), *Colomisphaera carpathica* (Borza), *Colomisphaera pieniniensis* (Borza) (Fig. 5.3), *Schizosphaerella minutissima* (Colom), filaments, ostracods, crinoids, aptychi, *Involutina* sp., and rare *Saccocoma* sp. It is noteworthy that some of the calpionellids and dinocysts mentioned above (*Colomisphaera pieniniensis* and *Stomiosphaera moluccana*) have never previously been observed in Upper Tithonian units (Reháková 2000), and *Praetintinnopsella andrusovi* has only been seen rarely (in the lower *Crassicollaria* Zone, with *T. remanei* and uncommon *C. alpina*). We surmise that they were re-sedimented.

Crassicollaria Zone, Intermedia Subzone (*sensu* Remane et al. 1986) — samples CH206–CH41

Biomicrite limestones have calpionellid-globochaete-radiolarian, calpionellid-radiolarian, radiolarian-calpionellid-globochaete, globochaete-calpionellid, calpionellid-globochaete and radiolarian-calpionellid microfacies (wackestones) make-ups. It contains calcified radiolarians, sponges, globochaetes and diverse calpionellid associations including *Calpionella*

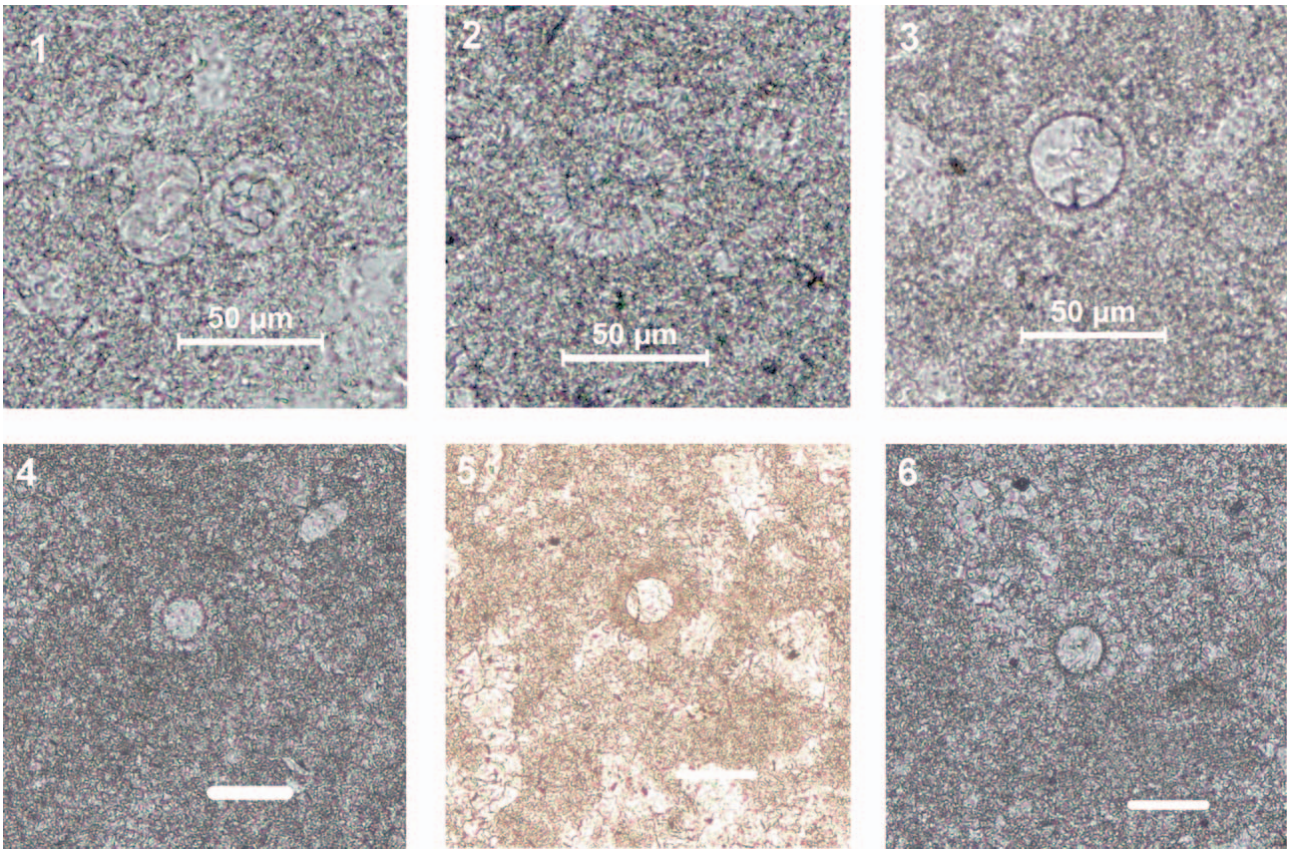

Fig. 6. 1 — *Stomiosphaera moluccana* Wanner; Sample CH202. **2** — *Colomisphaera nagyi* (Borza); Sample CH203. **3** — *Colomisphaera pieniniensis* (Borza); Sample CH205. **4** — *Schizosphaerella minutissima* (Vogler); Sample CH50. **5** — *Cadosina semiradiata fusca* Wanner; Sample CH47. **6** — *Colomisphaera carpathica* (Borza); Sample CH20. Scale bars in Figs. 4–6 are 50 µm.

alpina Lorenz, *Calpionella grandalpina* Nagy, *Calpionella elliptalpina* Nagy, *Crassicollaria massutiniana* (Colom), *Crassicollaria parvula* Remane, *Crassicollaria brevis* Remane, *Tintinnopsella carpathica* (Murgeanu & Filipescu), cysts of *Stomiosphaerina proxima* Řehánek, *Schizosphaerella minutissima* (Colom), *Cadosina semiradiata fusca* Wanner, bivalve fragments, filaments, miliolid foraminifers, crinoids, aptychi and rare planktonic crinoids — *Saccocoma* sp. Some crassicollarian loricas are very thin and deformed.

Two limestone layers (samples CH33 and CH36) show pelbiomicrite to pelbiomicrosparite/pelbiosparite structure (packestones and grainstones, Fig. 8.6). They contain small pellets, frequent globochaetes, fragments of planktonic crinoids (*Sacccoma* sp.), crinoid columnals, less frequent agglutinated and hyaline foraminifers, bivalves, ostracods, calcified radiolarians and rare calpionellids and cysts mentioned above: *Calpionella alpina* Lorenz, *Calpionella grandalpina* Nagy, *Crassicollaria intermedia* (Durand Delga), *Crassicollaria parvula* Remane, *Crassicollaria massutiniana* (Colom), *Crassicollaria brevis* Remane, cysts of *Cadosina semiradiata fusca* Wanner and *Schizosphaerella minutissima* (Colom).

Crassicollaria Zone, Colomi Subzone (*sensu* Reháková & Michalík 1997) — samples CH42–CH46

Biomicrite limestones consist of calpionellid-globochaete, globochaete-calpionellid, calpionellid-radiolarian, radiolaria-calpionellid, and calpionellid-radiolarian-globochaete microfacies (wackestones to packstones). In some layers, crassicollarians increase in abundance, and some of them have thin and aberrant loricas (Fig. 8.5). Generally they contain frequent *Crassicollaria parvula* Remane, less common *Crassicollaria massutiniana* (Colom), rare *Crassicollaria brevis* Remane, *Crassicollaria colomi* Doben, *Calpionella alpina* Lorenz, *Calpionella grandalpina* Nagy, globochaetes, calcified radiolarians, fragments of planktonic *Saccocoma* sp., bivalves, ostracods, aptychi and infrequent cysts — *Cadosina semiradiata fusca* Wanner and *Schizosphaerella minutissima* (Colom) (Fig. 6.4).

This interval also contains layers with marks of re-sedimentation. Several of them (samples CH31, -59, -58, -56, -55 and -54) were investigated under the microscope. Some have fragments of *Saccocoma* sp., and crinoids dominate over foraminifers, ophiuroids, globochaetes, calpionellids and dinoflagellate cysts. On the other hand, pelbioclastic limestones (grainstones, Fig. 8.2) contain abundant pellets, globochaetes and the "acme" of the calpionellids *Calpionella alpina* Lorenz, *Calpionella grandalpina* Nagy, *Calpionella elliptalpina* Nagy (Fig. 5.6), *Tintinnopsella carpathica* (Murgeanu & Filipescu) (Fig. 8.3), *Crassicollaria intermedia* (Durand Delga) (Fig. 8.4), *Crassicollaria massutiniana* (Colom), *Crassicollaria parvula* Remane and *Crassicollaria brevis* Remane (Fig. 5.7). Many of the crassicollarian loricas are thin and deformed. *Cadosina semiradiata fusca* (Wanner), *Schizosphaerella minutissima* (Colom), calcified radiolarians, ostracods, crinoids, ophiuroids, bivalves, aptychi, agglutinated foraminifers and *Saccocoma* sp. are rare.

Calpionella Zone, Alpina Subzone (*sensu* Remane et al. 1986; Reháková & Michalík 1997; Lakova et al. 1999; Boughdiri et al. 2006 and Andreini et al. 2007) — samples CH101–CH1

Biomicrites (predominantly wackestones) in which the ratio of calpionellids, radiolarians and globochaetes determines the type of microfacies (calpionellid-globochaete-radiolarian, calpionellid-radiolarian (Fig. 7.1), radiolarian-calpionellid, calpionellid-globochaete and globochaete-calpionellid (Fig. 7.2)). The *Crassicollaria-Calpionella* zonal boundary may be placed between 101 and the next sample below. Sample CH101 contains predominantly spherical forms of *Calpionella alpina* Lorenz (Fig. 8.1), two loricas of *Crassicollaria parvula* Remane, calcified radiolarians and sponges, globochaetes and very infrequent fragments of echinoids and ostracods. Higher up, in the samples of biomicrite wackestone, there are infrequent *Crassicollaria brevis* Remane, *Calpionella grandalpina* Nagy, cysts of *Cadosina semiradiata fusca* Wanner (Fig. 6.5), *Schizosphaerella minutissima* (Colom), *Colomisphaera carpathica* (Borza) (Fig. 6.6), rare ostracods, bivalves, aptychi and filaments were observed. The stratigraphical range of the above mentioned calpionellids has thus far been seen as being limited to the Upper Tithonian (Reháková 2000).

Crassicollaria parvula Remane increases in abundance in samples CH113, -15, and -112. Here rare fragments of planktonic crinoids, *Saccocoma* sp., were also identified. Borza (1984), in a chart showing microfossil stratigraphic ranges, indicated that saccocomids never cross the J/K boundary. We confirm the same experience. Events of increased abundance of crassicollarians visible in some sections (Houša et al. 2004; Pruner et al. 2010) were interpreted as a *Crassicollaria parvula* "acme" zone ("CPAZ") or a potential "epibole". We suppose that this assemblage represented the Alpina Subzone of the standard *Calpionella* Zone of the Lower Berriasian (*cf.* Reháková & Michalík 1997), but it occasionally contains some older *Crassicollaria*, from Upper Tithonian limestones, incorporated into the micrite matrix of the Alpina Subzone. A more dynamic, more agitated, water-body regime in the Jurassic/Cretaceous boundary interval was documented by Olóriz et al. (1995), and recently also by Grabowski et al. (2010a), Michalík & Reháková (2011) and Reháková et al. (2011).

Frequent intercalations composed of pelbiomicrites passing to pelbiomicrosparites/pelbiosparites and breccia layers (packstones to grainstones) were observed also in this part of the sequence (Fig. 7.3). They usually contain abundant pellets, bioclasts and intraclasts, which contain spectra of typical Late Tithonian calpionellids (Fig. 6.6). The abundance of calpionellids and globochaetes in some of these intercalations is greater than the abundances visible in the biomicrite layers described above. *Calpionella alpina* Lorenz, *Calpionella grandalpina* Nagy, *Tintinnopsella carpathica* (Murgeanu & Filipescu), *Crassicollaria massutiniana* (Colom), *Crassicollaria parvula* Remane, *Crassicollaria colomi* Doben, and cysts of *Cadosina semiradiata fusca* Wanner, *Schizosphaerella minutissima* (Colom) and *Colomisphaera* sp. were recognized. Deformed crassicollarian

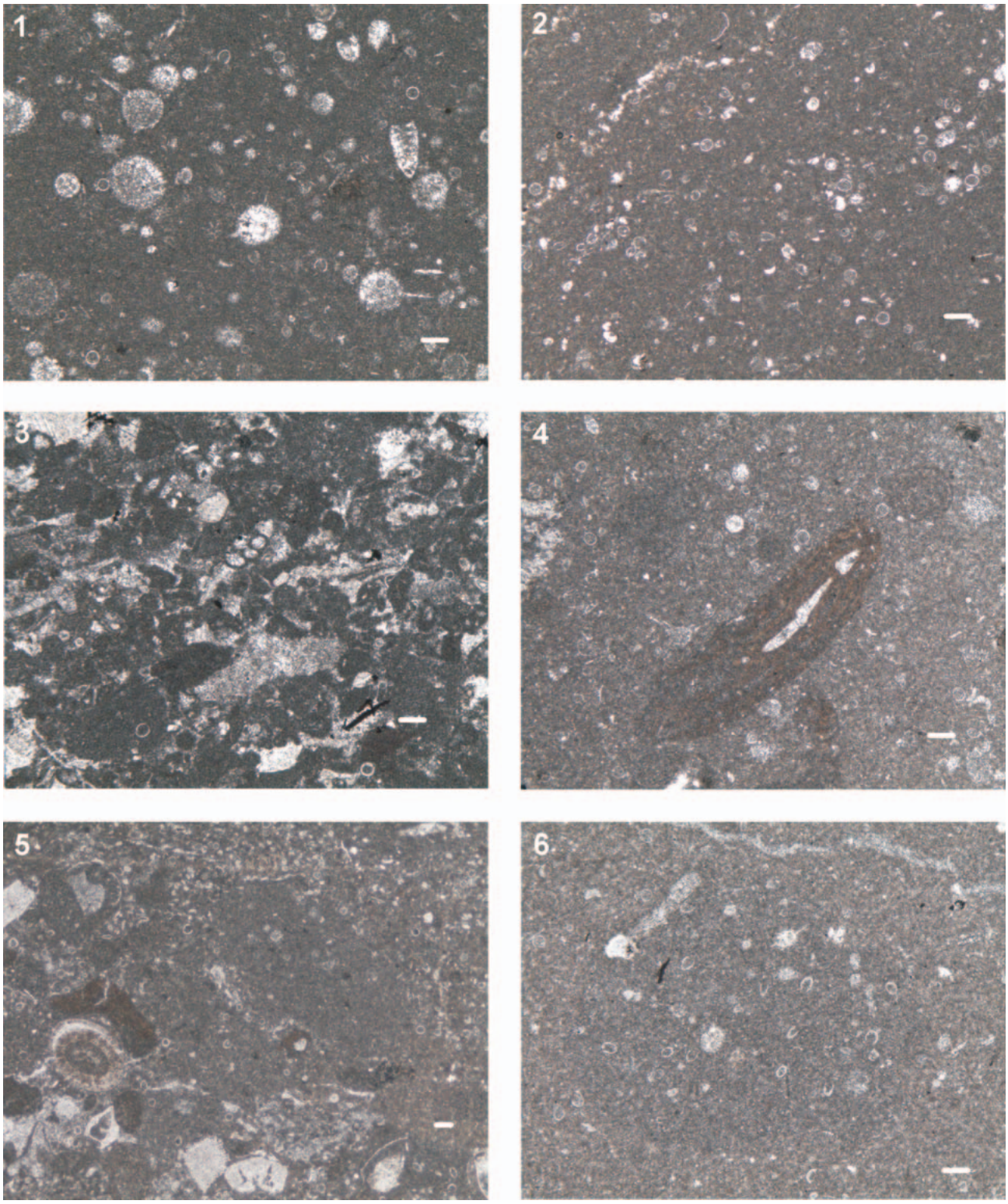

Fig. 7. 1 — *Calpionella*-radiolarian microfacies with calcified radiolarians and *Calpionella alpina* Lorenz; Sample CH6. **2** — Globochaete-*Calpionella* microfacies with *Calpionella alpina* and *Crassicollaria parvula*; Sample CH9. **3** — Microclastic limestone (grainstone) with *Calpionella alpina*, *Crassicollaria parvula*, agglutinated foraminifers, crinoids and bivalves; Sample CH14. **4** — *Crescentiella morronensis* (Crescenti) in biomicrite limestone (wackestone); Sample CH17. **5** — Microclastic limestone (grainstone) with the extraclasts of calpionellid limestones, and biogenic fragments coming from shallow-water environments (ooids and bryozoans). **6** — Clast of biomicrite wackestones with more abundant crassicollarians (*Crassicollaria brevis*, *Crassicollaria parvula*) in microbrecciated limestone; Sample CH23. Scale bars in all figures are 100 μm.

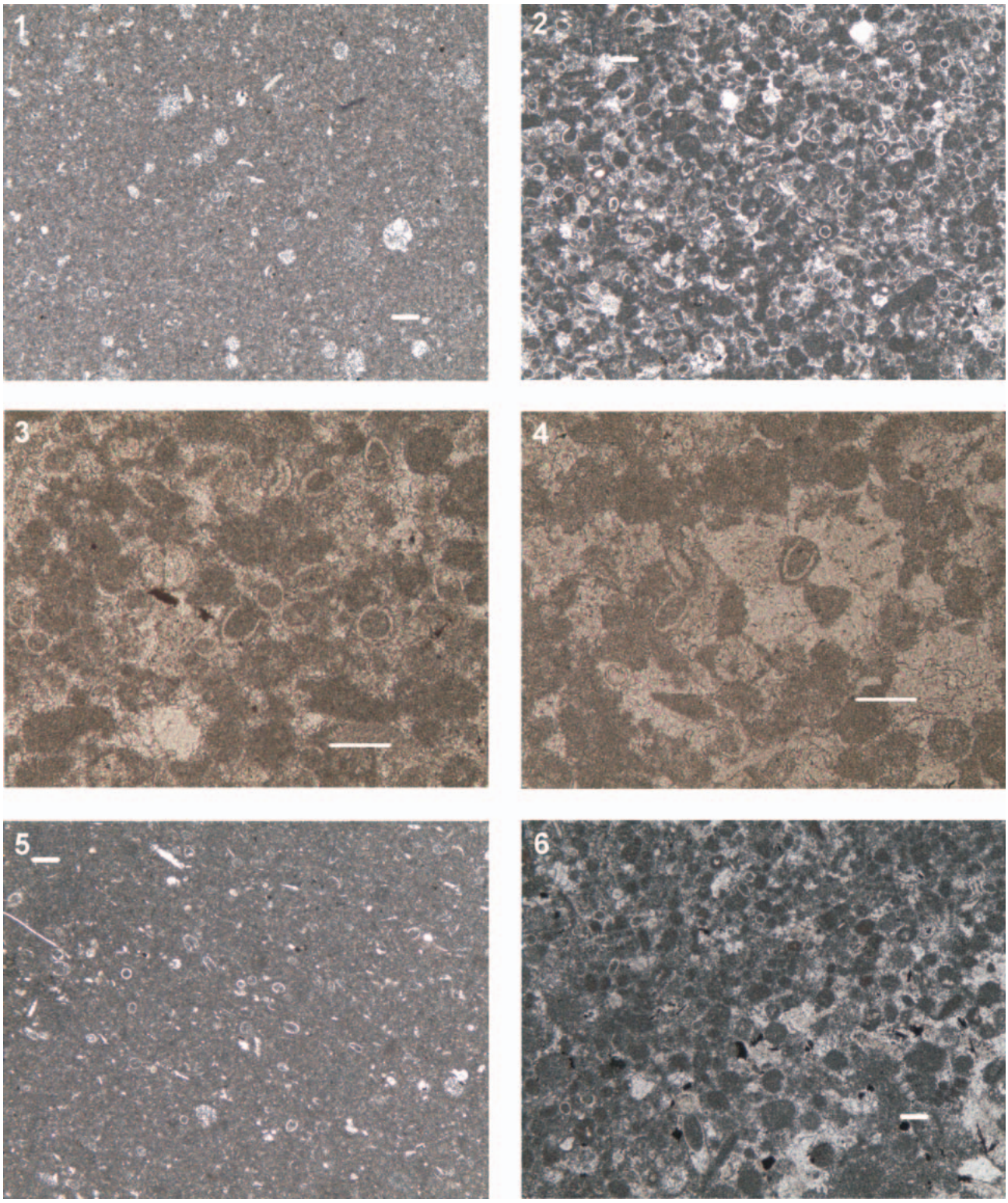

Fig. 8. 1 — Biomicrite limestone (wackestone) dominated by spherical forms of *Calpionella alpina*; Sample CH101. **2** — Pelbioclastic limestone (grainstone) with pellets, frequent calpionellids and rare benthic fragments (crinoids, bivalves, ophiuroids); Sample CH54. **3** — *Tintinnopsella carpathica* and common crassicollarians in pelbiomicrosparite limestone; Sample CH56. **4** — *Crassicollaria intermedia* in pelbiosparitic limestone in which *Saccocoma* sp., and benthic fragments dominated over rare calpionellids and globochaetes; Sample CH58. **5** — Biomicrite limestone of *Calpionella*-globochaete microfacies with common calpionellids. Some of the crassicollarian loricas are thin and aberrant; Sample CH61. **6** — Pelbiomicrosparite limestone with common *Saccocoma* sp., fragments of foraminifers, bivalves, ostracods and also rare calpionellids, cysts, radiolarians and globochaetes; Sample CH33. Scale bars in all figures are 100 μm.

loricas are still present. Benthos is represented by crinoids, ophiuroids, echinoid spines, agglutinated foraminifers, *Textularia* sp., *Lenticulina* sp. and ostracods; there are also uncommon *Saccocoma* sp. (Fig. 7.3). Bioclasts coming from more shallow-water environments, such as *Crescentiella morronensis* (Crescenti) (Fig. 7.4), *Bacinella irregularis* Radoičić, ooids (Fig. 7.5), and fragments of bryozoans and algae, have also been identified.

The sequence studied is composed of Upper Tithonian-Lower Berriasian limestones (peloidal wackestone/packstone, graded bioclastic grainstones, wackestones/packstones with ramp-derived intraclasts and bioclasts, marly limestones with intraclasts and limestone pebbles), sedimented in an outer ramp environment periodically influenced by storms/or small-scale sea-level fluctuations, reflected in inputs of coarser materials.

Comments on calpionellid stratigraphy

Three calpionellid zones have been recognized: the *Chitinoidella* Zone, *Crassicollaria* Zone and *Calpionella* Zone. The middle part of that interval contains Late Tithonian taxa: *Tintinnopsella remanei*, *Tintinnopsella carpathica*, *Crassicollaria intermedia*, *Crassicollaria massutiniana*, *Crassicollaria brevis*, *Crassicollaria parvula*, *Crassicollaria colomi*, *Calpionella alpina*, and *Calpionella grandalpina*. The pelbiomicrites and microbreccia layers recognized there are composed of abundant taxa typical of the Intermedia Subzone (*Crassicollaria* Zone). The lowermost intercalations, with abundant *Saccocoma* sp., show indications of storm sedimentation, during which there were sudden inputs of saccocomids — identifiable in the rock by their chaotic orientation and intimate mixing with peloids.

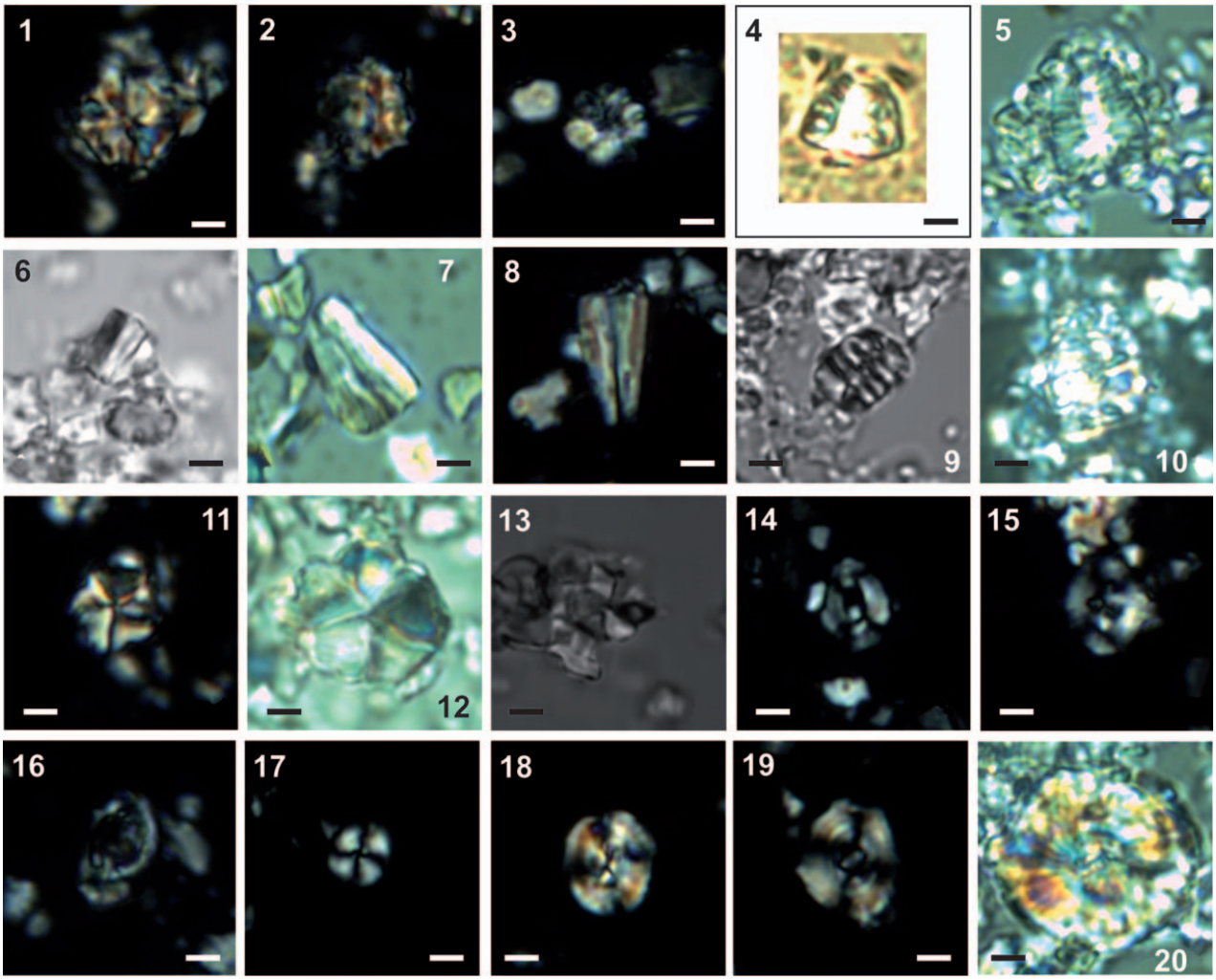

Fig. 9. Selected nannofossil taxa. Scale bar represents 2 μm. **1** — *Nannoconus* sp. Side view (SV); Sample CH47. **2** — *Nannoconus erbae*; Sample CH45. **3** — *Nannoconus globulus minor*; Sample CH56. **4** — *Nannoconus wintereri*; Sample CH15. **5** — *Nannoconus kamptneri minor*; Sample CH15. **6** — *Conusphaera mexicana minor*; Sample CH203. **7** — *Conusphaera mexicana mexicana*; Sample CH101. **8** — *Conusphaera mexicana mexicana*; Sample CH37. **9** — *Faviconus multicolumnatus*; Sample CH204. **10** — *Nannoconus steinmannii minor*; Sample CH15. **11** — Pentalith; Sample CH45. **12** — Pentalith; Sample CH47. **13** — *Hexalithus noeliae*; Sample CH17. **14** — *Microstaurus chiastius*; Sample CH37. **15** — *Cruciellipsis cuvillieri*; Sample CH45. **16** — *Rhagodiscus asper*; Sample CH25. **17** — *Cyclagelosphaera margerelii*; Sample CH37. **18** — *Watznaueria barnesiae*; Sample CH37. **19** — *Watznaueria britannica*; Sample CH56. **20** — *Watznaueria manivitiae*; Sample CH204.

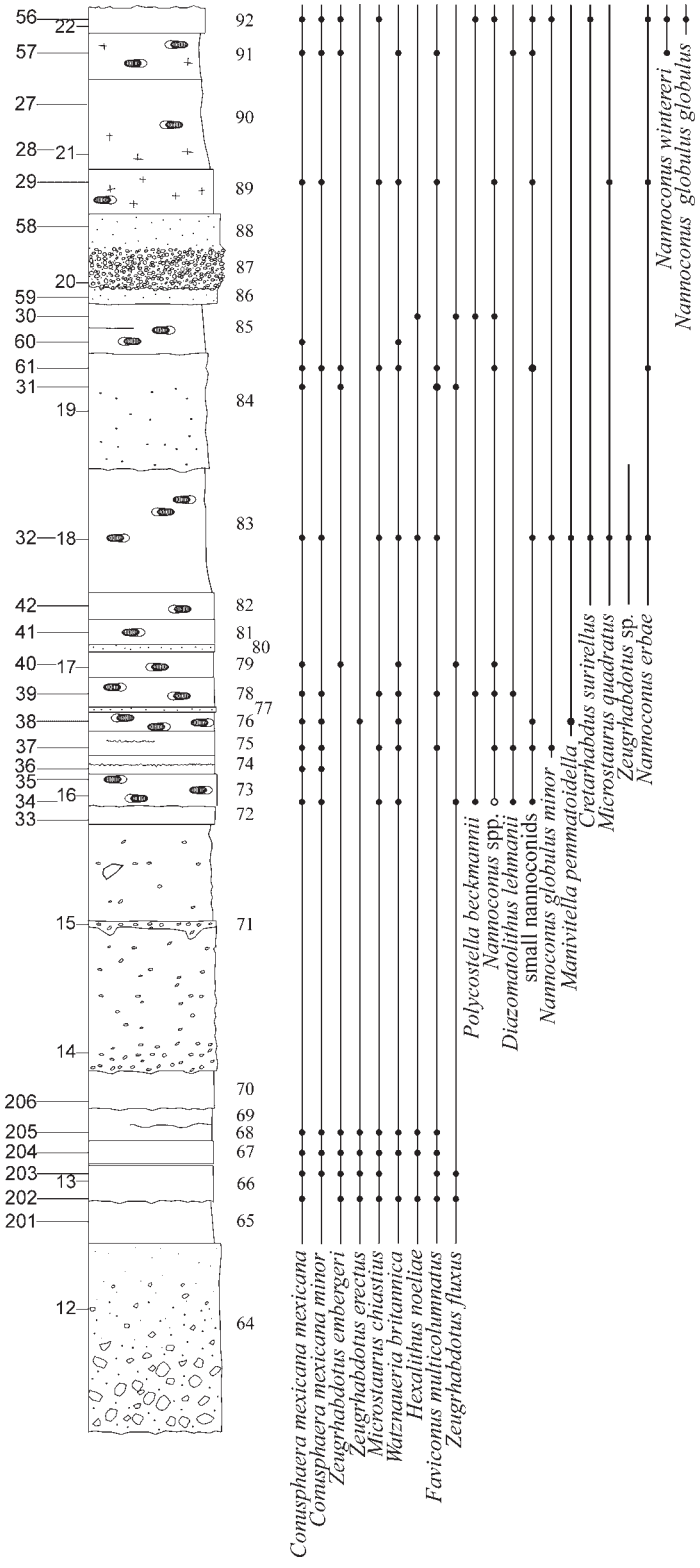

Fig. 10. Vertical ranges of selected calcareous nannofossils in beds 66–92. Open circles denote an uncertain specific identification.

The approximate Jurassic/Cretaceous boundary, the onset of the Alpina Subzone of the standard *Calpionella* Zone, is located in sample CH101 (bed 100). There, globochaetes and calcified radiolarians dominate over medium-sized spherical forms of *Calpionella alpina* (accompanied by infrequent *Crassicollaria parvula*) in biomicrites of the calpionellid-radiolaria-globochaete microfacies. Thus, the base of the Alpina Subzone corresponds to that described by Remane et al. (1986). Those authors noticed (but did not explain) the sudden rapid decrease in calpionellid abundance. A quantitative analysis of bio-elements shows that their decrease coincided with an increase of radiolarians. The upper part of the sequence, composed of wackestones, has yielded Early Berriasian taxa (*Calpionella alpina*, *Crassicollaria parvula* and *Tintinnopsella carpathica*). Pelbiomicrite/pelbiosparite and bioclastic intercalations show different spectra of redeposited bio-fragments. If compared with autochthonous deposits, their calpionellid associations (with double or triple abundances) are composed predominantly of spherical *Calpionella alpina*, with less frequent to common *Crassicollaria parvula*. Thus, the "acme" of calpionellids in this section represents a rather enriched taphocenosis, one linked with depositional dynamics resulting in the reworking and transport of sediments. This is also supported by the presence of ooids, agglutinated foraminifers, *Bacinella irregularis* Radoičić, *Crescentiella morronensis* (Crescenti) — elements typical of the shoals of inner ramp environments.

Microfacies, calpionellid associations and their distribution at the J/K boundary allow some comparisons between key sites. For instance, the interval at Le Chouet resembles those known from the Puerto Escaño section (Pruner et al. 2010) and the Caravaca, Rio Argos section (Michalík & Reháková 2011). The calpionellids of the Bosso Valley section (Houša et al. 2004) show similarities with those at Brodno (Houša et al. 1999; Michalík et al. 2009). On the other hand, microfacies as well as calpionellid distribution at Torre de'Busi (Casellato et al. 2008) are very similar to those known from the Nutzhof section (Lukeneder et al. 2010).

Calcareous nannofossils

A total of 64 samples for calcareous nannofossil biostratigraphic investigation have been examined. Biostratigraphic analyses were performed on simple smear slides, prepared as follows: a small amount of rock material was powdered adding a few drops of bi-distillated water; the obtained suspension was mounted onto a microscope slide, covered with a slide cover and fixed with Norland Optical Adhesive, without centrifuging, ultrasonic cleaning or settling of the sediment — in order to retain the original composition. The smear slides were then inspected using a light-polarizing microscope, at 1250× magnification. Calcareous nannofossils were documented using a MicroPublisher 5.0 RTV camera (Dept. Earth Sciences "A. Desio", Università degli Studi di Milano, Milan) and a LEICA DFC 290 HD camera (Dept. of Geology and Paleontology, Comenius University, Bratislava).

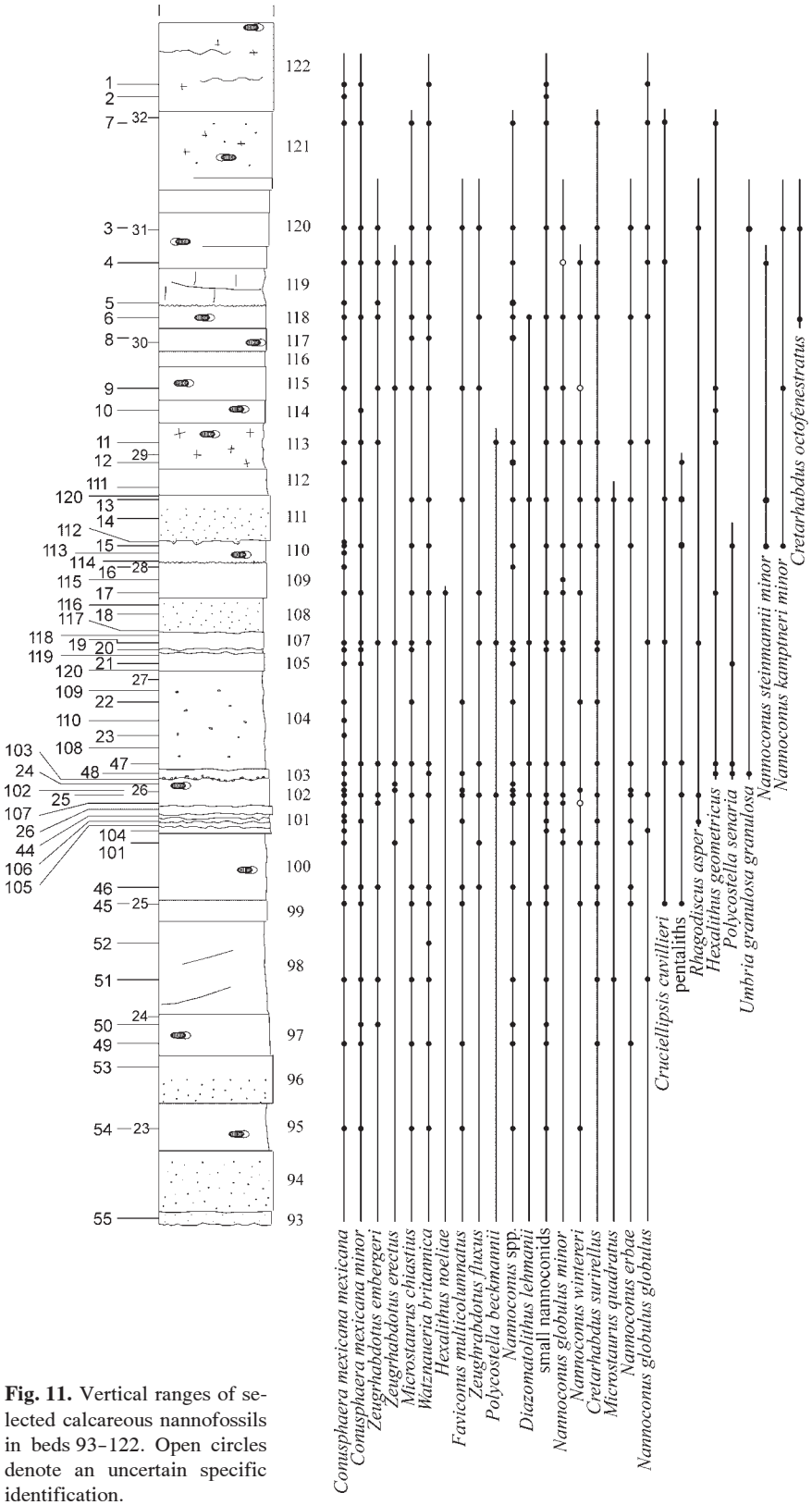

Fig. 11. Vertical ranges of selected calcareous nannofossils in beds 93–122. Open circles denote an uncertain specific identification.

In the samples studied, calcareous nannofossils are rare to common and very poorly to poorly preserved. They are affected by overgrowth and etching phenomena, and observed associations are often dominated by dissolution-resistant species (principally the genera *Watznaueria*, *Cyclagelosphaera* and *Conusphaera*) (Roth 1986). Nevertheless, the events suggested as useful in constraining the Jurassic/Cretaceous boundary (Wimbledon et al. 2011) have been detected, namely the first occurrences of: *N. wintereri* (in bed 91; Fig. 9.4), *C. cuvillieri* (bed 99; Fig. 9.15) and *N. steinmannii minor* along with *N. kamptneri minor* (bed 110; Fig. 9.10 and Fig. 9.5, respectively). A full list of the calcareous nannofossil taxa found in this study (genera, species and subspecies) is given below in an Appendix, in alphabetical order. The distribution of stratigraphically useful nannofossil taxa is shown in Figures 10 and 11.

Comments on calcareous nannofossil biostratigraphy

Calcareous nannofossil associations and their distribution in the J/K boundary interval at Le Chouet are consistent with calcareous nannofossil data reported from other key sites, such as Torre de'Busi, Brodno and Lokut. In particular, even though calcareous nannofossils are badly preserved, a few events present here have positions, relative to magnetozones and calpionellid zones, that are comparable to those at other localities. The first appearances of *N. wintereri* and *C. cuvilleri* are in the lower and lower-middle part of M19n, and the *Crassicollaria* Zone, respectively, as in the Torre de'Busi and Brodno sections. The first occurrences of *N. steinmannii minor* and *N. kamptneri minor* occur in the topmost part of the section, the uppermost part of M19n and *Calpionella* Zone, again consistent with data from Torre de'Busi and Lokut. Thus these events represent reliable data useful for long-range correlations, at least in low-latitude regions. The integrated results indicate that the first occurrences of *N. wintereri*, *C. cuvillieri*, *N. steinmannii minor* and *N. kamptneri minor* all occur in the *Berriasella jacobi* Subzone, a situation different to that previously reported by Bralower et al. (1989), who showed *N. wintereri* and *C. cuvillieri* as first appearing in the uppermost part of the *Durangites* Zone. The nannofossil zonation of Casellato (2010) is applied in Fig. 18.

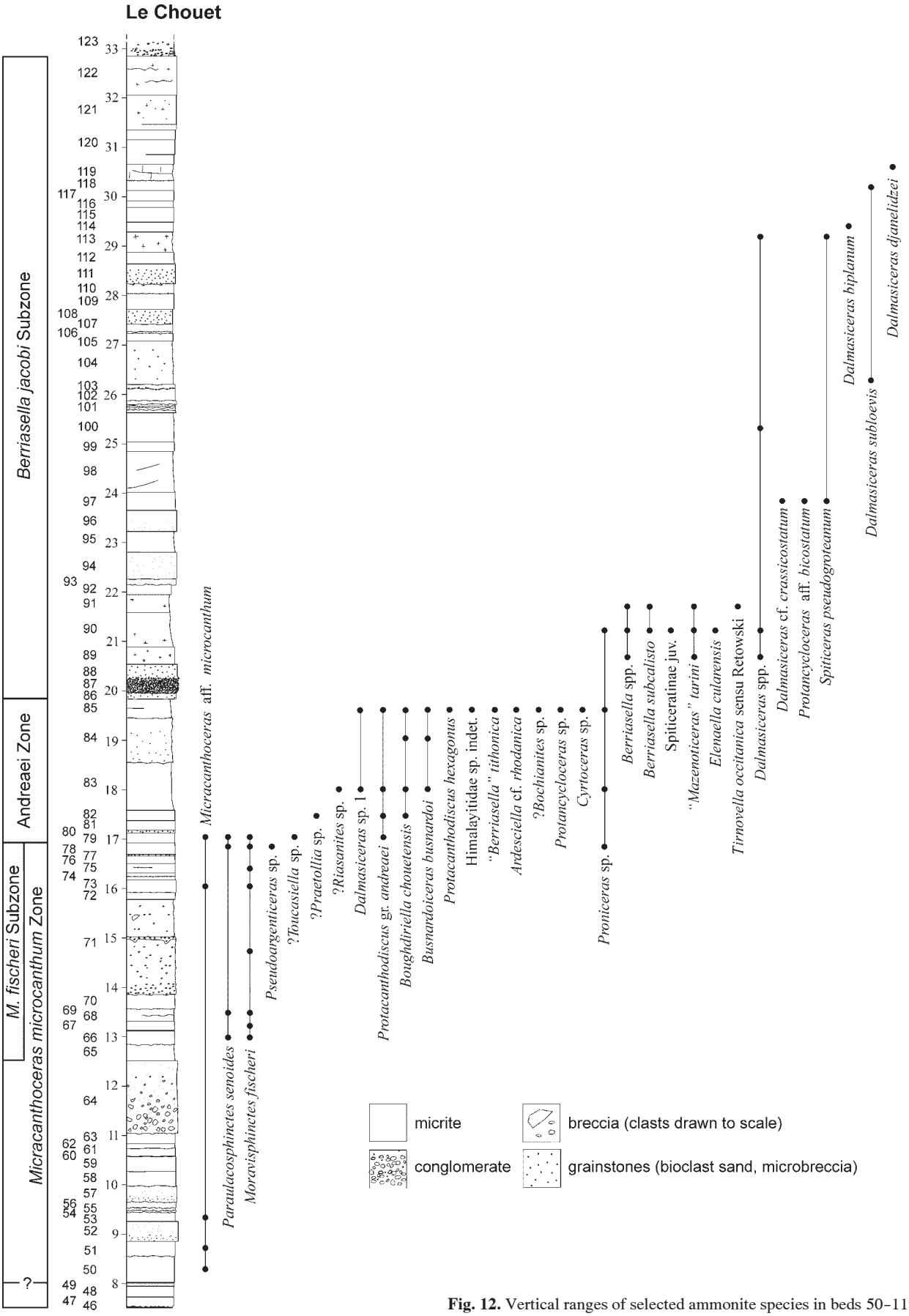

Fig. 12. Vertical ranges of selected ammonite species in beds 50–119.

Ammonites

The ammonite occurrences at Le Chouet are diverse. We have collected abundant material bed by bed, with 22 genera recognized, and our preliminary ammonite results provide a new biostratigraphical record for the Tithonian-Berriasian interval.

Figure 12 shows the vertical ranges of ammonite taxa, with the exception of common haploceratid, lytoceratid and phylloceratid species. A more detailed account of the ammonite fauna (with new taxa) will be published later, but as a synthesis of first results, the following may be related. In summary, four successive faunal assemblages can be recognized.

Micracanthoceras microcanthum Zone

At Le Chouet, the *Micracanthoceras microcanthum* Zone (Upper Tithonian) may be clearly recognized, though its base cannot be fixed precisely due to the lack of specimens below bed 50. Alongside the ammonite index, *M. microcanthum*, Phylloceratina and Lytoceratina predominate below, but just above a thick breccia (bed 64), the assemblage is composed essentially of *Paraulacosphinctes senoides* Tavera and *Moravisphinctes fischeri* Kilian, whereas *Micracanthoceras* becomes scarce.

Our first results thus suggest a partition of the *Microcanthum* Zone, with the establishment of a *Moravisphinctes fischeri* Subzone at the top, with its base at bed 66. This is used as a replacement for the Transitorius Zone, as already suggested (Cecca et al. 1989) in the type area for the Ardescian, and by authors in other Mediterranean marginal areas (Benzaggagh & Atrops 1997).

The last occurrence of the genus *Moravisphinctes* is located below the top of the *Crassicollaria intermedia* calpionellid Subzone. These results are in disagreement with findings from Morocco (Benzaggagh & Atrops 1997), where *Moravisphinctes* spp. last occurs in the Remanei Subzone.

Recognition of a fauna indicating the *Simplisphinctes* Subzone at the base of *M. microcanthum* Zone has not been possible and this requires further study. Thus, the current understanding of the *Microcanthum* Zone is an interval between the first occurrence of the index species (*sensu* Benzaggagh & Atrops 1997) and the first appearance of the genus *Protacanthodiscus* (in bed 79), which marks the next ammonite biostratigraphic unit, a zonal boundary, in calpionellid terms, still within the Intermedia Subzone.

Protacanthodiscus andreaei Zone

In its first appearances, specimens of *Protacanthodiscus* gr. *andreaei* (Kilian) are few in number, and its acme is seen in beds 83 to 85: a similar pattern of distribution to that which has been observed in Spain (Olóriz & Tavera 1989). The *Protacanthodiscus* gr. *andreaei* interval is a short one, whose top is affected by small-scale sedimentary reworking, though all within the lower part of the *C. colomi* Subzone.

The much-quoted "*Durangites* Zone" of the topmost Tithonian should be re-examined and perhaps abandoned because of the possibility that this genus may be endemic to the Mexican-Cuban region. Here we use a local index for the zone, *Protacanthodiscus andreaei.* The peak for *P. andreaei* coincides with the acme of *Busnardoiceras,* a common Lower Berriasian genus (first occurrence in bed 83), previously restricted by Le Hégarat to the *B. jacobi* and *P. grandis* Subzones. A new genus, *Bougdiriella* (type species *B. chouetensis* gen. and sp. nov., which we intend to describe separately) also appears in bed 82. This species has in the past usually been indentified as a Mediterranean "*Durangites*". We also intend to create a new genus, *Ardesciella*, for a group of Mediterranean species formerly assigned to *Corongoceras*, as suggested by Parent et al. (2011). The richness of the ammonite fauna of the Andreaei Zone at the genus level is a good faunal marker for this interval on all the margins of the Mediterranean Tethys.

?*Riasanites* sp. and ?*Praetollia* in the Andreaei Zone are reported for the first time in southern France. Both have traditionally been seen as typical boreal genera (Mitta 2007). The first, however, has been recorded in Tethyan Crimea (apparently in an equivalent of the *Berriasella picteti* Subzone: Kvantaliani & Lysenko 1979), in Yemen (*M. microcanthum* Zone: Howarth 1998) and in Argentina (Koeneni Zone: Zeiss & Leanza 2011) — thus, levels that stratigraphically bracket the Le Chouet occurrence. But the levels in Argentina, Yemen and at Le Chouet are all much older than the mid to Late Berriasian age of the type *Riasanites* zones in the Russian Platform embayment (? = *D. dalmasi* Subzone–*B. picteti* Subzone).

Berriasella jacobi Subzone

The first "Berriasian" ammonite assemblage appears here one third of the way up the *C. colomi* calpionellid Subzone. Though the index species has not been recognized yet, we maintain a *Berriasella jacobi* Subzone, for stability of stratigraphic nomenclature. The base of the *B. jacobi* Subzone at Le Chouet is marked by an increase in the numbers of morphospecies of *Dalmasiceras* (see Fig. 12), as observed by Le Hégarat (1971). This work provides the first recognition of the *Eleanella cularensis* horizon (Tavera et al. 1994) near the base of the *B. jacobi* Subzone. It is established that the base of the *B. jacobi* Subzone here does not correspond to the base of the calpionellid Alpina Subzone. In fact, none of the ammonite zonal boundaries correspond to any calpionellid boundaries. The grainstone–conglomerate–grainstone triplet that apparently coincides with the base of the Jacobi Subzone (Fig. 12) perhaps indicates some hiatus. However, the two massive breccias at lower levels, both with large angular clasts and irregular bases, may indicate more significant phases of erosion.

The boundary interval of the Tithonian–Berriasian generally shows clear losses at the family level, with the progressive decline of Himalayitidae in the highest Tithonian, replaced by berriasellids at the base of the Berriasian: what Wiedmann (1973) called the "the Tethysian boundary". As stated, this turnover is not synchronous with the *Crassicollaria/Calpionella* turnover used to define the base of the Alpina Subzone. The gap in phylogenetic knowledge and the

conglomerate bed (bed 87) complicate a perception of the magnitude of the ammonite turnover at Le Chouet. It is worth noting that other fossil groups pass this level with no change: no taxon of calpionellid or calcareous nannofossil appears or disappears in beds 86–88.

Magnetostratigraphy

The section at Le Chouet complies with our aims in three fundamental criteria, it has: (a) essentially continuous sedimentation, uninterrupted by marked diastems, (b) rich fossil associations (calpionellids, ammonites) allowing its detailed biostratigraphic division, and (c) rocks with magnetic properties that are favourable for reliable determination of paleomagnetic polarity.

Paleomagnetic properties of pilot samples

Our study has thus far concentrated on the pilot investigation of a 30 m-thick portion of the section of the limestone strata near the J/K boundary (beds 1–121). The average sampling density for the whole section is about three samples per metre of true stratal thickness.

Paleomagnetic measurements were performed in the Paleomagnetic Laboratory of the Institute of Geology, Prague. Remanent magnetization (RM) of the rocks was measured using a Liquid helium-free Superconducting Rock Magnetometer, type 755 4K SRM, and the magnetic susceptibility of the samples was measured using a KLY-4 Kappabridge (Jelínek 1966, 1973). The samples were demagnetized by alternate field (AF) in an Automatic Sample Degaussing System 2G600, reaching 100 mT. Thermal demagnetization (TD)

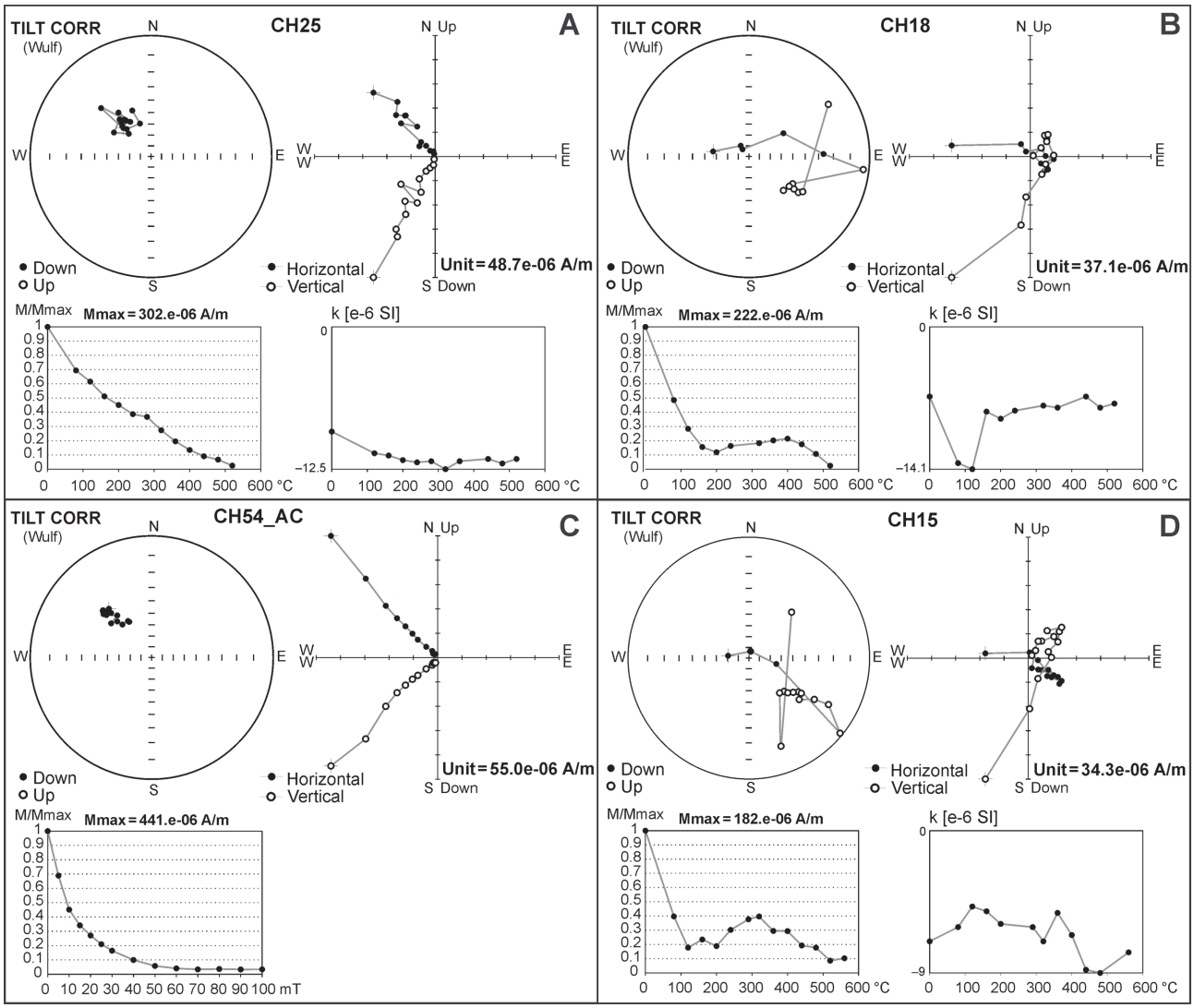

Fig. 13. Thermal (**A, B** and **D**) and AF demagnetization (**C**) of typical specimens. Top left diagrams: stereographic projection of demagnetization paths; full (open) symbols — lower (upper) hemisphere projection; top right diagrams: orthogonal projections of demagnetization paths (Zijderveld diagrams) on horizontal and vertical planes; bottom left diagrams: NRM intensity decay during demagnetization (M/Mmax); bottom right diagrams: susceptibility (k) changes during thermal treatment (A, B and D). Stereographic and orthogonal projections after tilt correction.

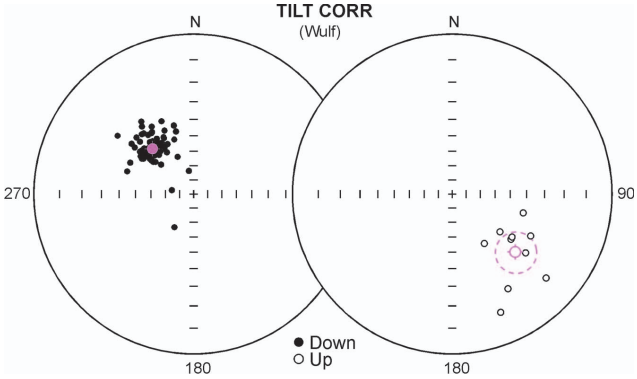

Fig. 14. Stereographic projection of the component C (after tectonic correction). **Left** — normal polarity directions, **right** — reversed polarity directions.

was performed in a non-magnetic oven placed in a Magnetic Vacuum System (MAVACS). The ambient magnetic field in the cooling chamber of the MAVACS demagnetizer did not exceed 1 nT, owing to a built-in rotating-coil magnetometer controlling the currents in its Helmholtz coil system (Příhoda et al. 1989). Processing of the output data, including, for instance, multicomponent analysis of the demagnetization path, was carried out using Remasoft 3.0 software (Chadima & Hrouda 2006).

Each of the 91 samples studied was subjected to TD or AF demagnetization in 12–13 temperatures or fields. Of the 91 samples, 83 yielded reliable paleomagnetic directions. As a result, the individual components could be precisely established in the majority of samples using a multicomponent analysis of remanence (Kirschvink 1980). Zijderveld diagrams and diagrams of normalized remanent values vs. labo-

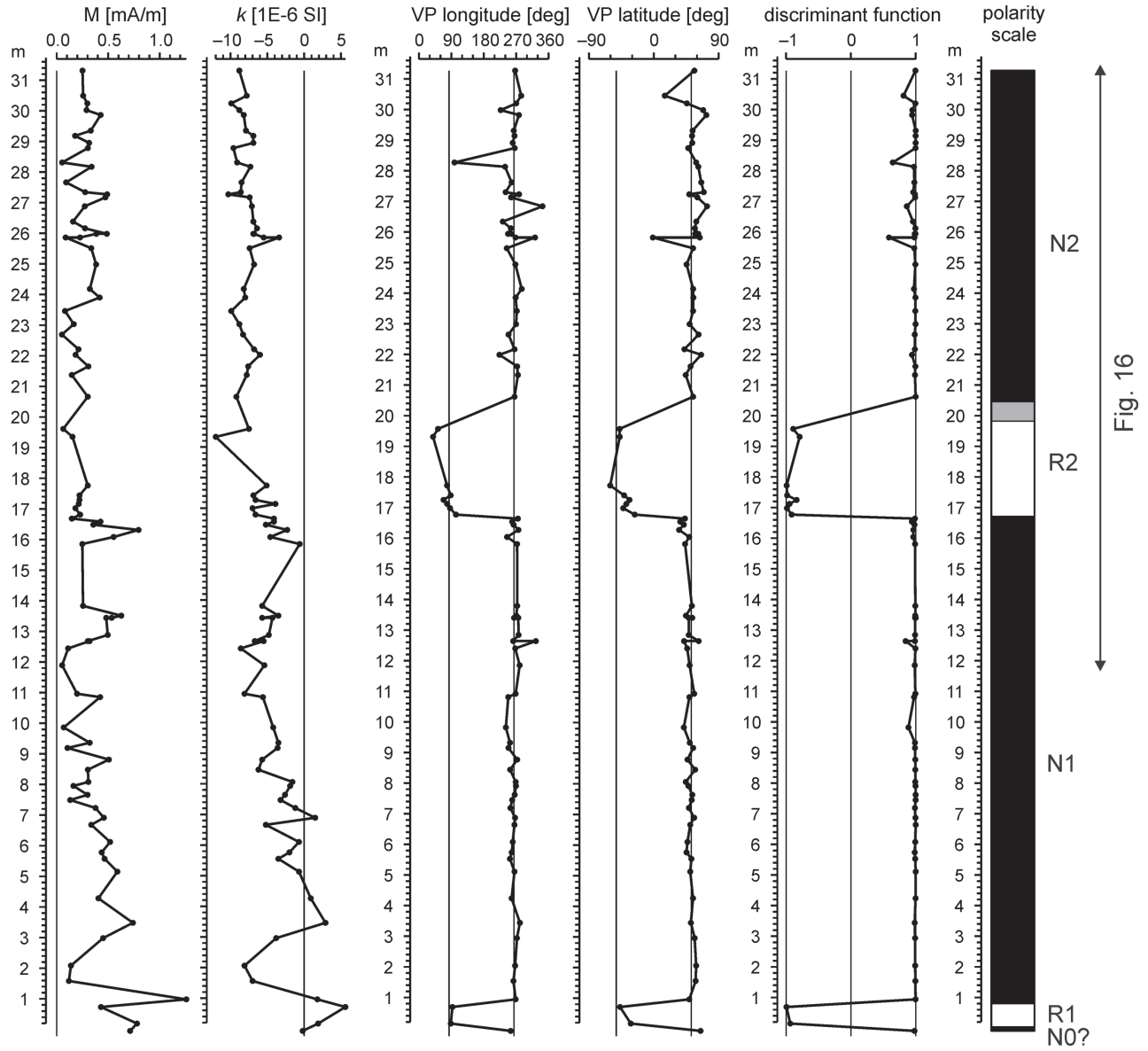

Fig. 15. Magnetostratigraphic profile through the Le Chouet section. **M** — remanent magnetization in natural state, **k** — volume magnetic susceptibility in natural state, **VP** — virtual pole. Magnetic polarity: **black** — normal, **white** — reversed. Grey indicates uncertain or mixed polarity.

ratory thermal demagnetizing field t (°C) were constructed for all samples.

The results of thermal (TD) and alternating field (AF) demagnetization procedures are displayed in Figure 13. They refer to two limestone samples with normal paleomagnetic directions (samples CH25 and CH54, from level 20.71 m in bed 89, and 31.18 m in bed 120, respectively) and two limestone samples with reverse paleomagnetic directions (samples CH15 and CH18, 17.07 m (bed 79) and 17.49 m (bed 82)). Analogous results were obtained for most samples through the Le Chouet section. The RM directions shown in the projections are corrected for the dip of the strata. The results of the multi-component analysis of remanence show that the rock samples display a two or three-component remanent magnetization. The A-component is undoubtedly of viscous origin and is demagnetizable in the temperature range of 20–120 °C (or AF 0–10 mT); the B-component is also of secondary origin, but shows 'harder' magnetic properties, being demagnetizable in a temperature range of 120–240 °C (or AF 10–15 mT); the C-component is the most stable, being demagnetizable in an unblocking temperature-range of ca. 400–520 °C (or AF unblocking fields 20–60 mT).

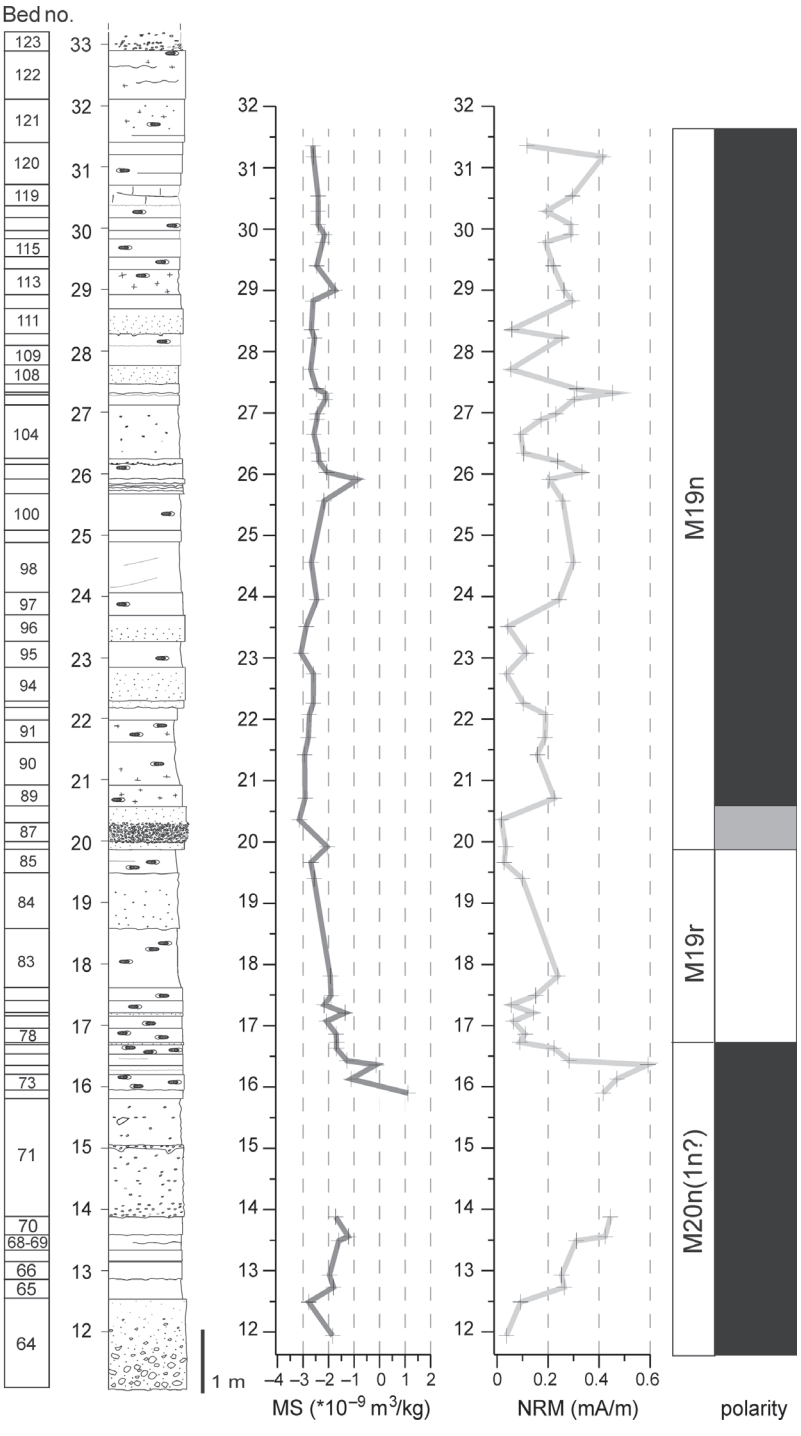

Fig. 16. Magnetostratigraphy and rock magnetic parameters: mass normalized magnetic susceptibility (MS) and natural remanent magnetization (NRM) intensity, from bed 64 upwards.

The mean directions and dispersions of components were calculated using Fisher's statistics (Fisher 1953) and were displayed on a Wulf stereographic projection. They are marked either by infilled or empty crossed circles, with a confidence circle circumscribed around the mean direction at the 95% probability level. Both magnetic polarities are present in the C-component directions. Consequently, after tectonic correction, the mean direction for samples with 'normal' polarity is D = 317.7°, I = 48.1°, α_{95} = 2.5°, and for those with reverse polarity it is D = 132.6°, I = –33.7°, α_{95} = 10.2° (Fig. 14). The paleolatitude (ca. 27°N) is in agreement with that obtained from the Berriasian type section (Galbrun 1985). Paleodeclination at Le Chouet implies a counterclockwise rotation of ca. 20–30°, which must be attributed to a local tectonic effect. The resulting magnetostratigraphic profile is shown in Fig. 15, displaying the following quantities: the modulus of natural remanent magnetization (*M*), volume magnetic susceptibility of samples in natural state (*k*), co-ordinates of the virtual pole position (VP longitude and VP latitude), and a discriminant function defining the polarity. Both the virtual pole position and the discriminant function are functions of the direction of the remanence C-component, and have been inferred by means of a multi-component analysis. As indicated in Fig. 15, normal (N) and reverse (R) polarity intervals, magnetozones and submagnetozones, are clearly manifested in the interpreted values of VP longitude and VP latitude and a discriminant function defining the polarity (Man 2008).

Low-field magnetic susceptibility (k) ranges from –12.0 to 5.6×10^{-6} SI and the intensity of the natural remanent magnetization (NRM) varies between 0.018 and 1.145×10^{-3} A/m.

These data given in the magnetostratigraphic profile indicate a gradual decrease in magnetization, from the older to the younger rocks (Fig. 15). An obvious decrease in these values up sequence in the vicinity of the J/K boundary has also been observed at Brodno, in the Bosso Valley and at Puerto Escaño (Houša et al. 1999, 2004; Pruner et al. 2010) as well as in sections from the Tatra (Central Carpathians — Grabowski & Pszczółkowski 2006) and the Transdanubian mountains (Lókút section — Grabowski et al. 2010b).

Discussion of the main magnetostratigraphic results

The preliminary magnetostratigraphic investigation of the basal 30 m of the profile, the measurement of basic magnetic properties and the results of multi-component analysis of remanence of the J/K boundary limestones have yielded new information on the correlation of paleomagnetic events with biozones, and with events elsewhere in Tethys. Magnetozones N0–N2 and R1–R2 (Fig. 15) might be roughly correlated to the Global Polarity Time Scale (GPTS). The correlation between magnetostratigraphy and calpionellid zonation in the J/K boundary interval is reliably tested in more than 20 land sections (see Ogg & Lowrie 1986; Channell et al. 1987; Ogg et al. 1991; Houša et al. 1999; Pruner et al. 2010; Grabowski 2011). Magnetozone N2, where the *Crassicollaria*/*Calpionella* zonal boundary is situated (see Fig. 16), must be correlated with magnetozone M19n (magnetosubzone M19n.2n). Reversed magnetozone R2 falls within the *Crassicollaria* Zone and should be interpreted as M19r. The sedimentation rate amounted to 10–15 m/Myr in the M19n–M19r interval. Magnetostratigraphic interpretation of the lower part of the section poses some problems. Bed 33 and approximately bed 60 belong to the *Chitinoidella* Zone. Magnetozone N1 might correspond to M20.1n, while N0 might be taken to be the topmost part of M20n.2n. However, interpretation of R1 as magnetosubzone M20n.1r is not straightforward. Its biostratigraphic position below the documented *Chitinoidella* Zone would deviate substantially from that in the Brodno and Puerto Escaño sections (there in the lowermost part of the *Crassicollaria* Zone — see Houša et al. 1999; Pruner et al. 2010). It might be compared with the Bosso valley section, where M20n.1r does occur in the middle part of the *Chitinoidella* Zone (Houša et al. 2004). However, interpretation of the R1 polarity interval as M20n.1r would imply a very high sedimentation rate in the *Chitinoidella* Zone and lower *Crassicollaria* Zone, at almost 50 m/Myr: a great contrast with sedimentation rates calculated for the upper *Crassicollaria* and Alpina Zones. Alternatively, the interval N1 might be interpreted as the whole of magnetozone M20n, and R1 as M20r. However, R1 is apparently too thin to be M20r (ca. 1 m) and this would imply a dramatic decrease in the sedimentation rate — no more than 1.5 m/Myr.

The next step in the paleomagnetic investigation will be a more refined determination of the magnetostratigraphic boundaries, with special emphasis on documentation of the short reversed magnetosubzones M20n.1r and M19n.1r. The average sampling density for the whole section should be

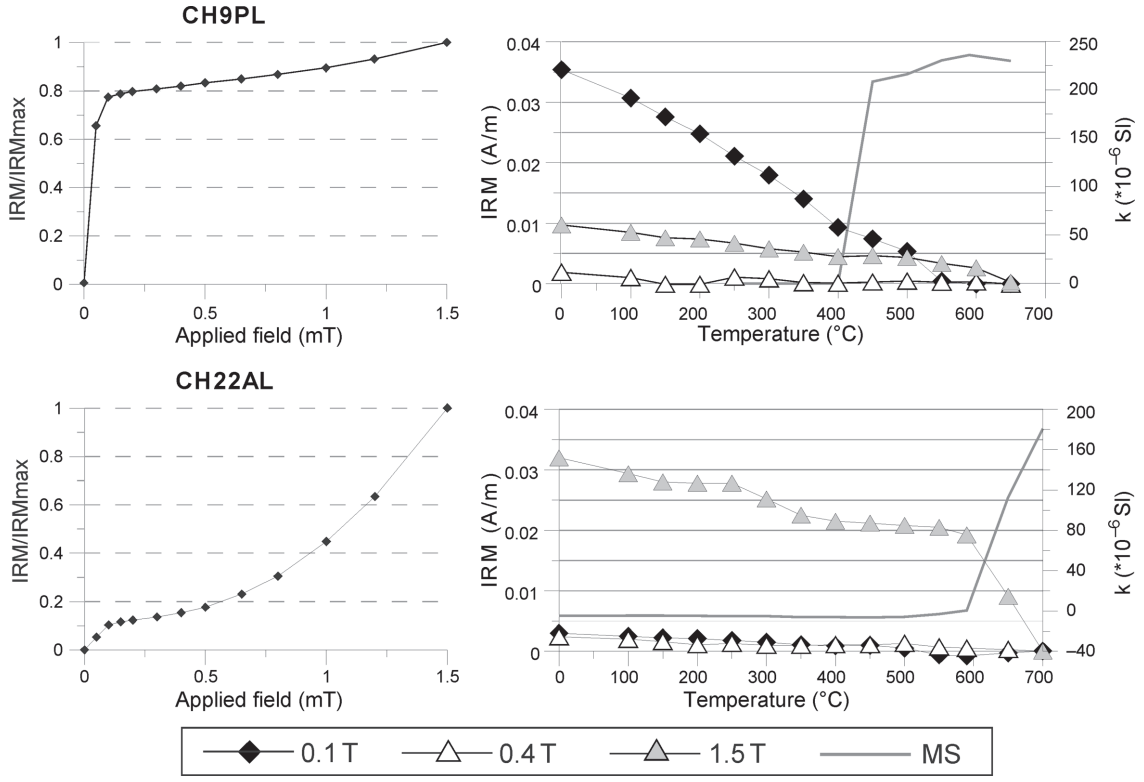

Fig. 17. Isothermal remanent magnetization (IRM) acquisition curves, thermal demagnetization of the 3 axes IRM acquired in the fields of 0.1 T, 0.4 T and 1.5 T and volume magnetic susceptibility (k) changes during thermal treatment for selected samples. Upper row: sample CH9PL (bed 73, 16.13 m). Lower row: sample CH22AL (bed 86, 19.92 m).

about 5–8 per metre, with 20 or more samples per metre at critical levels such as zonal boundaries.

Rock magnetism

Basic rock magnetic investigations were performed for all the horizons sampled for magnetostratigraphy. They were carried out in the Paleomagnetic Laboratory of the Polish Geological Institute–National Research Institute and included measurements of mass normalized magnetic susceptibility (MS) and isothermal remanent magnetization (IRM) acquired in the field of 1 T along the Z-axis of the cylindrical specimen and then anti-parallel in the field of 100 mT. The S-ratio calculated as a ratio of IRM intensities acquired in both fields was an indicator of proportions of low and high coercivity minerals. Selected samples with contrasting S-ratios were subjected to stepwise IRM acquisition and thermal demagnetization of 3 axes IRM (acquired in the fields of 0.1 T, 0.4 T and 1.5 T in three perpendicular directions) in order to identify magnetic minerals by recognition of their unblocking temperature spectra (Lowrie 1990). The detailed results of a rock magnetic study will be presented in a future paper, thus they are summarized here only briefly.

Both low- and high-coercivity minerals are present throughout the section (Fig. 17). The low-coercivity mineral is interpreted as magnetite, as its maximum unblocking temperature is between 550° and 600 °C. A high-coercivity mineral with maximum unblocking temperatures between 600° and 700 °C (hematite) is also present. Magnetite-dominated samples (like CH9PL in Fig. 17) contain the primary component C. Hematite-dominated samples (like CH22AL in Fig. 17) typically occur in brecciated and detrital horizons. Hematite does not carry any natural remanence, therefore it is most probably a product of secondary (diagenetic) oxidation.

Conclusion

We here calibrate calpionellid, nannofossil, ammonite and magnetostratigraphic data in this interval (Fig. 18).

The base of the *Calpionella* Zone (Alpina Subzone) is located within M19n.2n, which is consistent with its position relative to magnetostratigraphy at, for instance, Puerto Escaño and Lókút, though not at Brodno (*sensu* Michalík et al. 2009). At Le Chouet, the base and top of the Andreaei Zone are within M19r, whereas at Puerto Escaño the "*Durangites* Zone" is reported as straddling M20n, M19r and the lowest part of M19n.2n.

A series of nannofossil first-appearance datums has been recognized (Fig. 18), as follows: *Nannoconus globulus minor* (16.38 m), *Cretarhabdus surirellus* and *Nannoconus erbae* (18.00 m), *N. wintereri* (21.80 m), *N. globulus globulus* (22.05 m), *Cruciellipsis cuvillieri* (25.00 m), *N. steinmanni minor* and *N. kamptneri minor* (28.15 m). The base of the *Calpionella alpina* Zone, with its predominance of small globular *C. alpina*, is bracketed between the FADs of *Nannoconus wintereri* and *N. globulus globulus* and that of *N. steinmanni minor* and *N. kamptneri minor*, and the FAD of *Cruciellipsis cuvillieri* lies about half a metre below the zonal boundary. The Upper Jurassic to Lower Cretaceous sequence at Le Chouet may be compared to other well-documented sites with intervals that cross the J/K boundary (Fig. 19).

Acknowledgments: Many colleagues helped us in this work, with both moral and practical support. We thank three reviewers for their stimulating suggestions. Thanks are due to Mgr Stanislav Šlechta and Ing. Tadeusz Sztyrak for field

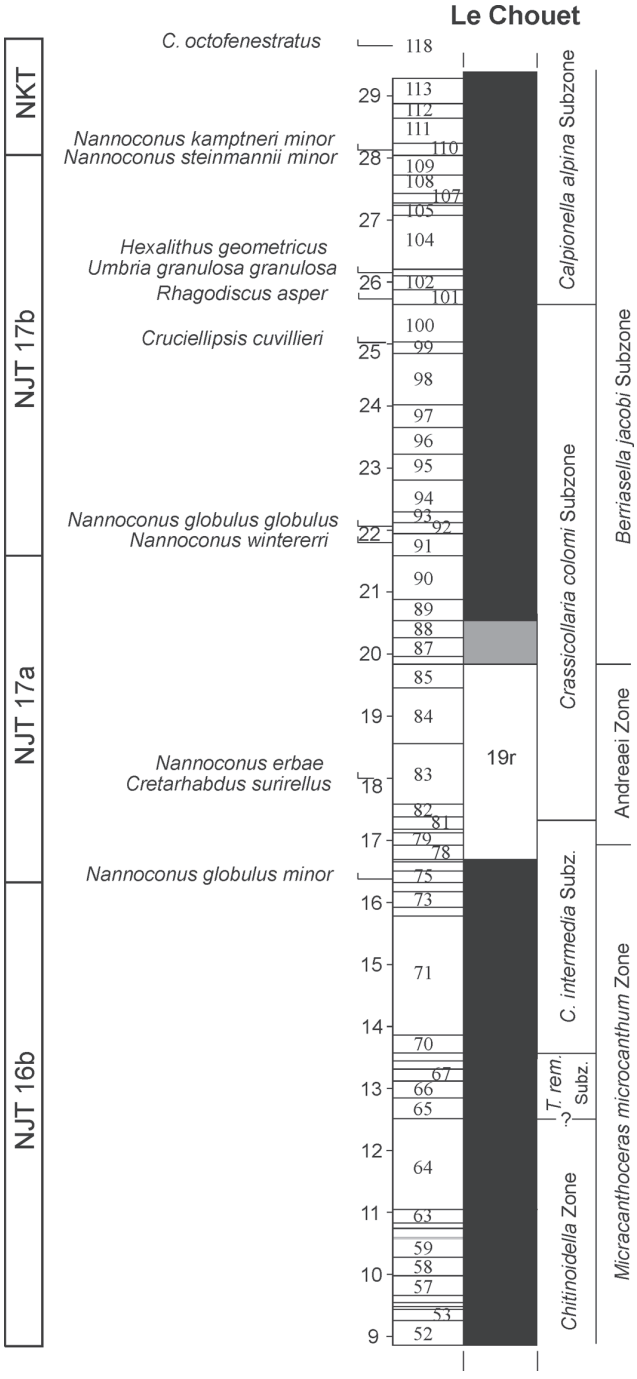

Fig. 18. Calibration of magnetozonal and biozonal (ammonite, calpionellid) boundaries and selected FADS for calcareous nannofossils at Le Chouet. Nannofossil zones follow Casellato (2010). Grey in the magnetozone column indicates uncertain or mixed polarity.

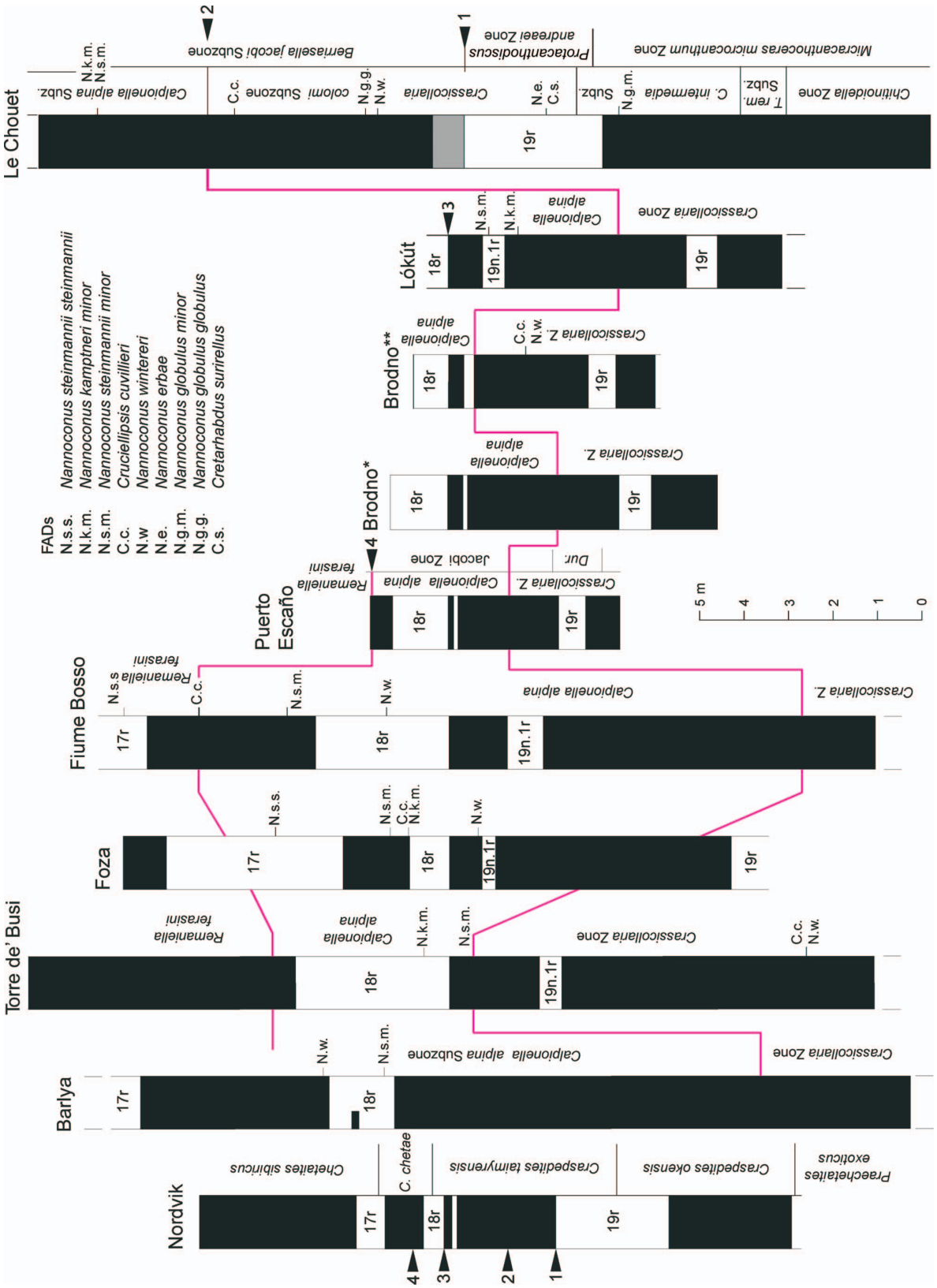

Fig. 19. Correlation of selected sequences showing the M20–M17 interval. Revised from Wimbledon et al. (2011). Brodno columns based on data in ** Michalík et al. (2009) and *Houša et al. (2009). Data 1–4 in Tethys (base of *B. jacobi* Subzone, base of Alpina Subzone, top of M19n.2n, and base of Ferasini Subzone) and their approximate positions at Nordvik (column after Houša et al. 2007). The Barlya column is based on data provided by Platon Tchoumatchenco (unpublished magnetozones by B. Galbrun). Lókút after Grabowski et al. (2010b).

assistance. Paleomagnetic analyses were performed by Dr Daniela Venhodová, Mrs Jana Drahotová and Mr Jiří Petráček. Software for evaluation of paleomagnetic measurements was prepared by Dr Ota Man. We thank Dr Platon Tchoumatchenco, Institute of Geology BAS, Sofia, for his contribution of unpublished data on Barlya. PP and PS gratefully acknowledge the Research Plan of the IG AS CR No. CEZ AV0Z30130516 for financial support. They also acknowledge support from the Institute of Geology ASCR, v.v.i. through its internal Project 9342 "Magnetostratigraphy and magnetomineralogy of the J/K boundary interval on the Le Chouet, St. Bernard's Spring and Barlya sites". JG and KS were financially supported by the Polish-French bilateral cooperation Project No. 683/N-POLONIUM/2010/0. This is also a contribution to projects of the Slovak Grant Agency: APVV-0280-07, APVV-0644-10, LPP 0120-09 and VEGA grant 2/0042/12 and VEGA 2/0068/11. We thank Gloria Andreini and colleagues in the University of Perugia for their essential help processing calpionellid samples from the lower part of the section. CEC warmly thanks the Micropaleontology Research Group, Università degli Studi di Milano, and specifically Prof. E. Erba, for continuous support.

References

Andreini G., Caracuel J.E. & Parisi G. 2007: Calpionellid biostratigraphy of the Upper Tithonian–Upper Valanginian interval in Western Sicily (Italy). *Swiss J. Geosci.* 100, 179–198.

Bacelle L. & Bosellini A. 1965: Diagrammi per la stima visiva della composizione perventualle nelle rocce sedimentarie. *Ann. Univ. Ferrara, N.S., Sez. IX., Sci. Geol. Paleont.* 1, 59–62.

Benzaggagh M. & Atrops F. 1997: Stratigraphie et associations de faune d'ammonites des zones du Kimméridgien, Tithonien et Berriasien basal dans le Prérif interne (Rif, Maroc). *Newslett. Stratigr.* 35, 127–163.

Borza K. 1984: The upper Jurassic–Lower Cretaceous parabiostratigraphic scale on the basis of Tintinninae, Cadosinidae, Stomiosphaeridae, Calcisphaerulidae and other microfossils from the West Carpathians. *Geol. Zborn. Geol. Carpath.* 35, 539–550.

Boughdiri M. 1994: Les genres d'ammonites *Durangites* et *Protacanthodiscu*s (Tithonien superieur) dans la Tethys occidentale (SE Espagne, SE France, Algerie et Tunisie). *Stratigraphie, Paleontologie, Biogeographie, These, Univ. Claude-Bernard-Lyon I*, 351–94.

Boughdiri M., Sallouhi H., Maâlaoui K., Soussi M. & Cordey F. 2006: Calpionellid zonation of the Jurassic-Cretaceous transition in north Atlasic Tunisia. Updated Upper Jurassic stratigraphy of the "Tunisian Trough" and regional correlations. *Compt. Rendus Geosci.* 338, 1250–1259.

Bown P.R. & Cooper M.K.E. 1998: Jurassic. In: Bown P.R. (Ed.): Calcareous nannofossil biostratigraphy. *Kluwer Academic Publishers*, Cambridge, 34–85.

Bralower T.J., Monechi S. & Thierstein H.R. 1989: Calcareous nannofossils Zonation of the Jurassic-Cretaceous Boundary interval and correlations with the Geomagnetic Polarity Timescale. *Mar. Micropal.* 14, 153–235.

Casellato C.E. 2010: Calcareous nannofossil biostratigraphy of Upper Callovian-Lower Berriasian successions from Southern Alps, North Italy. *Riv. Ital. Paleont. Stratigr.*116, 357–404.

Casellato C.E., Andreini G., Erba E. & Parisi G. 2008: Calcareous Nannofossil and Calpionellid calcification events across the Tithonian-Berriasian time interval and low latitudes paleoceanographic implications. Proceedings of 12th INA, Lyon, France, 7–11 September 2008. *J. Nannoplankton Res., Spec. Publ.*, 33–33.

Cecca F., Enay R. & Le Hégarat G. 1989: L'Ardescien (Tithonique supérieur) de la région stratotypique: série de référence et faunes (ammonites, calpionelles) de la bordure ardéchoise. *Doc. Lab. Géol. Lyon* 107, 1–115.

Chadima M. & Hrouda F. 2006: Remasoft 3.0 — A user-friendly palaeomagnetic data browser and analyzer. *Travaux Géophysiques* XXXVIII, 20–21.

Channell J.E.T., Casellato C.E., Muttoni G. & Erba E. 2010: Magnetostratigraphy, nannofossil stratigraphy and apparent polar wander for Adria-Africa in the Jurassic-Cretaceous boundary interval. *Palaeogeogr. Palaeoclimatol. Palaeoecol.* 293, 51–75.

Détraz H. & Mojon P.O. 1989: Evolution paléogeographique de la marge jurassiene de la Tethys du Tithonique-Portlandien au Valanginien: correlations biostratigraphique et sequentielle des facies marins a continentaux. *Eclogae Geol. Helv.* 82, 37–112.

Enay R., Boughdiri M. & Le Hégarat G. 1998: *Durangites, Protacanthodiscus* (Ammonitina) et formes voisines du Tithonien superieur — Berriasian dans la Tethys mediterreenne (SE France, Espagne, Algerie et Tunisie). *C.R. Acad. Sci. Paris* 327, 425–430.

Fisher R. 1953: Dispersion on a sphere. *Proc. Roy. Soc.* A 217, 295–305.

Galbrun B. 1985: Magnetostratigraphy of the Berriasian stratotype section (Berrias, France). *Earth Planet. Sci. Lett.* 74, 130–136.

Grabowski J. 2011: Magnetostratigraphy of the Jurassic/Cretaceous boundary interval in the Western Tethys and its correlations with other regions: a review. *Volumina Jurassica* 9, 105–128

Grabowski J. & Pszczółkowski A. 2006: Magneto- and biostratigraphy of the Tithonian-Berriasian pelagic sediments in the Tatra Mountains (central Western Carpathians, Poland): sedimentary and rock magnetic changes at the Jurassic/Cretaceous boundary. *Cretaceous Research* 27, 398–417.

Grabowski J., Michalík J., Pszczółkowski A. & Lintnerová O. 2010a: Magneto- and isotope stratigraphy around the Jurassic/Cretaceous boundary in the Vysoká Unit (Malé Karpaty Mts, Slovakia): correlations and tectonic implications. *Geol. Carpathica* 61, 309–326.

Grabowski J., Haas J., Márton E. & Pszczółkowski A. 2010b: Magneto- and biostratigraphy of the Jurassic/Cretaceous boundary in the Lókút section (Transdanubian Range, Hungary). *Stud. Geophys. Geodet.* 54, 1–26.

Grandesso P. 1977: Gli strati a Precalpionellidi del Titoniano e I loro raporti conil Rosso Ammonitico Veneto. *Mem. Sci. Geol.* 32, 1–15.

Houša V., Krs M., Krsová M., Man O., Pruner P. & Venhodová D. 1999: High-resolution magnetostratigraphy and micropaleontology across the J/K boundary strata at Brodno near Žilina, western Slovakia: summary results. *Cretaceous Research* 20, 699–717.

Houša V., Krs M., Man O., Pruner P.,Venhodová D., Cecca F., Nard G. & Piscitello M. 2004: Combined magnetostratigraphic, paleomagnetic and calpionellid investigations across Jurassic/Cretaceous boundary strata in the Bosso Valley, Umbria, central Italy. *Cretaceous Research* 25, 771–785.

Houša V., Pruner P., Zakharov V.A., Košťák M., Chadima M., Rogov M.A., Slechta S. & Mazuch M. 2007: Boreal-Tethyan Correlation of the Jurassic-Cretaceous boundary interval by magneto- and biostratigraphy. *Stratigr. Geol. Correlation* 15, 297–309.

Howarth M.K. 1998: Tithonian and Berriasian ammonites from the Chia Gara Formation of northern Iraq. *Palaeontology* 35, 597–655.

Jan du Chęne R. , Busnardo R., Charollais J., Clavel B., Deconinck J.-F., Emmanuel L., Gardin S., Gorin G., Manivit H., Monteil E., Raynaud J.-F., Renard M., Steffen D., Steinhauser N.,

Strasser A., Strohmenger C. & Vail P.R. 1993: Sequence-stratigraphic interpretation of Upper Tithonian-Berriasian reference sections in South-East France: a multidisciplinary approach. *Bull. Cent. Rech. Expl.-Prod. Elf Aquitain* 17, 1, 151–181.

Jelínek V. 1966: A high-sensitivity spinner magnetometer. *Stud. Geophys. Geodaet.* 10, 58–78.

Jelínek V. 1973: Precision A.C. bridge set for measuring magnetic susceptibility and its anisotropy. *Stud. Geophys. Geodaet.* 17, 36–48.

Joseph P., Beaudoin B., Sempéré T. & Maillart J. 1988: Vallées sous-marines et systemes d'épandage carbonatés du Berraisien vocontien (Alpes méridionales francaises). *Bull. Soc. Géol. France* 4, 363–374.

Joseph P., Beaudoin B., Fries G. & Parize O. 1989: Les vallées sous-marines enregistrent au Crétacé inférieur le fonctionnement en blocs basculés du domain vocontien. *C.R. Acad. Sci. Paris* 309, 1031–1038.

Kirschvink J.L. 1980: The least-squares line and plane and the analysis of palaeomagnetic data. *Geophys. J. Roy. Astron. Soc.* 62, 699–718.

Kvantaliani I.V. & Lysenko N.I. 1979: On the problem of a Berriasian zonation in Crimea. *Soobsch. Akad. Nauk. Gruz. SSR* 94, 629–632.

Lakova I., Stoykova K. & Ivanova D. 1999: Calpionellid, nannofossils and calcareous dinocyst bioevents and integrated biochronology of the Tithonian to Valanginian in the West Balkan Mountains, Bulgaria. *Geol. Carpathica* 50, 151–168.

Le Hégarat G. 1971: Le Berriasian du sud-est de France. *Doc. Lab. Geol. Fac. Sci. Lyon* 43, 1, 1–308.

Lowrie W. 1990: Identification of ferromagnetic minerals in a rock by coercivity and unblocking temperature properties. *Geophys. Res. Lett.* 17, 159–162.

Lukeneder A., Halásová E., Kroh A., Mayrhofer S., Pruner P., Reháková D., Schnabl P., Sprovieri M. & Wagreich M. 2010: Multistratigraphic investigations of the Jurassic-Cretaceous boundary interval in the Gresten Klippenbelt (Austria) — evidence for depositional and evolutionary events. *Geol. Carpathica* 61, 365–381.

Maillard G. 1884: Invertébrés du Purbeckien du Jura. *Mém. Soc. Paléont. Suisse* 11, 1–156.

Man O. 2008: On the identification of magnetistratigraphic polarity zones. *Stud. Geophys. Geodaet.* 52, 173–186.

Mazenot G. 1939: Le Paléohoplitidae tithoniques et Berriasiens du Sud-est de la France. *Mém. Soc. Géol. France* 41, 1–303.

Michalík J. & Reháková D. 2011: Possible markers of the Jurassic/Cretaceous boundary in the Mediterranean Tethys — A review and state of art. *Geosci. Frontiers* 2, 475–490.

Michalík J., Reháková D., Halásová E. & Lintnerová O. 2009: The Brodno section — potential regional stratotype of the Jurassic/Cretaceous boundary (Western Carpathians). *Geol. Carpathica* 60, 213–232.

Mitta V.V. 2007: Ammonite assemblages from basal layers of the Ryazanian Stage (Lower Cretaceous) of Central Russia. *Stratigr. Geol. Correlation* 15, 193–205.

Ogg J.G. & Lowrie W. 1986: Magnetostratigraphy of the Jurassic/Cretaceous boundary. *Geology* 14, 547–550.

Ogg J.G., Hasenyager R.W., Wimbledon W.A., Channell J.E.T. & Bralower T.J. 1991: Magnetostratigraphy of the Jurassic-Cretaceous boundary interval-Tethyan and English faunal realms. *Cretaceous Research* 1, 455–482.

Olóriz F. & Tavera J.M. 1989: The significance of Mediterranean ammonites with regard to the traditional Jurassic-Cretaceous boundary. *Cretaceous Research* 10, 221–237.

Olóriz F., Caracuel J.E., Marques B. & Rodríguez-Tovar F.J. 1995: Asociaciones de Tintinnoides en facies ammonitico rosso de la Sierra Norte (Mallorca). *Rev. Esp. Paleont.*, 77–93.

Parent H., Scherzinger A. & Schweigert G. 2011: The Tithonian-Berriasian ammonite fauna and stratigraphy of Arroyo Cieneguita, Neuquén-Mendoza Basin, Argentina. *Bol. Inst. Fisiografía Geol.* 79–81, 21–94.

Perch-Nielsen K. 1985: Mesozoic calcareous nannofossils. In: Bolli H.M., Saunders J.B. & Perch-Nielsen K. (Eds.): Plankton stratigraphy. *Cambridge University Press*, Cambridge, 329–426.

Pruner P., Houša V., Olóriz F., Košťák M., Krs M., Man O., Schnabl P., Venhodová D., Tavera J.M. & Mazuch M. 2009: High-resolution magnetostratigraphy and biostratigraphic zonation of the Jurassic/Cretaceous boundary strata in the Puerto Escaño section (southern Spain). *Cretaceous Research* 31, 192–206.

Příhoda K., Krs M., Pešina B. & Bláha J. 1989: MAVACS — a new system creating a nonmagnetic environment for palaeomagnetic studies. In: Banda E. (Ed.): Paleomagnetismo-palaeomagnetism, CSIC, Madrid, 1988–1989. *Cuadernos de Geologia Iberica*, 223–250.

Reháková D. 2000: Evolution and distribution of the Late Jurassic and Early Cretaceous calcareous dinoflagellates recorded in the Western Carpathians pelagic carbonate facies. *Miner. Slovaca* 32, 79–88.

Reháková D. & Michalík J. 1994: Abundance and distribution of late Jurassic-Early Cretaceous microplankton in Western Carpathians. *Geobios* 27, 135–156.

Reháková D. & Michalík J. 1997: Evolution and distribution of calpionellids — the most characteristic constituents of Lower Cretaceous Tethyan microplankton. *Cretaceous Research* 18, 493–504.

Reháková D., Matyja B.A., Wierzbowski A., Schlögl J., Krobicki M. & Barski M. 2011: Stratigraphy and microfacies of the Jurassic and Lowermost Cretaceous of the Veliky Kamenets section (Pieniny Klippen belt, Carpathians, Western Ukraine). *Volumina Jurassica* 9, 61–104.

Remane J. 1970: Die Entstehung der resedimentarun Breccien in Obertithon der subalpen Ketten Frankreiches. *Eclogae Geol. Helv.* 63, 685–740.

Remane J., Borza K., Nagy I., Bakalova-Ivanova D., Knauer J., Pop G. & Tardi-Filácz E. 1986: Agreement on the subdivision of the standard calpionellid zones defined at the IInd Planktonic Conference Roma 1970. *Acta Geol. Hung.* 29, 5–14.

Roth P.H. 1983: Jurassic and Lower Cretaceous calcareous nannofossil in the Western North Atlantic (Site 534): biostratigraphy, preservation and some observation on biogeography and paleoceanography. *Initial Reports of the Deep Sea Drilling Project*, Washington D.C. 76, 587–621.

Roth P.H. 1986: Mesozoic palaeoceanography of the North Atlantic and Tethys Oceans. In: Summerhays C.P. & Shackleton N.J. (Eds.): North Atlantic Paleoceanography. *Geol. Soc., Spec. Publ.* 26, 299–320.

Tavera J.M. 1985: Los ammonites del Tithonico superior-Berriasense de la zona Subbetica (Cordilleros beticas). *Thesis Doctoral Univerisdad Granada*, 1–379.

Tavera J.M., Aguado R., Company M. & Olóriz F. 1994: Integrated biostratigraphy of the Durangites and Jacobi zones (J/K boundary) at the Puerto Escaño section in southern Spain (province of Cordoba). *Geobios Mem. Spec.* 17, 469–476.

Wiedmann J. 1973: Evolution or revolution of ammonoids at Mesozoic system boundaries. *Biological Rev.* 48,159–194.

Wimbledon W.A.P., Casellato C.E., Reháková D., Bulot L.G., Erba E., Gardin S., Verreussel R.M.C.H., Munsterman D.K. & Hunt C. 2011: Fixing a basal Berriasian and Jurassic-Cretaceous (J-K) boundary — perhaps there is some light at the end of the tunnel? *Riv. Ital. Paleont. Stratigr.* 117, 295–307.

Zeiss A. & Leanza H. 2011: Upper Jurassic (Tithonian) ammonites from the lithographic limestones of the Zapala region, Neuquén Basin, Argentina. *Beringeria* 41, 1–52.

Appendix: Calcareous nannofossils

Authors and date of the original description and, where appropriate, emendations are provided. See Perch-Nielsen (1985), Bralower et al. (1989), Bown & Cooper (1998), Casellato (2010) and references therein for full information on taxonomy and authorships.

Conusphaera mexicana (Trejo, 1969) subsp. *mexicana* Bralower *in* Bralower et al., 1989
Conusphaera mexicana (Trejo, 1969) subsp. *minor* (Bown & Cooper, 1989) Bralower *in* Bralower et al., 1989
Cretarhabdus octofenestratus Bralower *in* Bralower et al., 1989
Cretarhabdus surirellus (Deflandre *in* Deflandre & Fert, 1954) Reinhardt, 1970
Cruciellipsis cuvillieri (Manivit, 1956) Thierstein, 1971
Cyclagelosphaera argoensis Bown, 1992
Cyclagelosphaera deflandrei (Manivit, 1966) Roth, 1973
Cyclagelosphaera margerelii Noël, 1965
Cyclagelosphaera riyadhensis Varol, 2006
Cyclagelosphaera tubulata (Grün & Zweili, 1980) Cooper, 1987
Diazomatolithus lehmanii Noël, 1965
Faviconus multicolumnatus Bralower *in* Bralower et al., 1989
Hexalithus geometricus Casellato, 2010
Hexalithus noeliae (Noël, 1956) Loeblich & Tappan, 1966
Manivitella pemmatoidea (Deflandre *ex* Manivit, 1965) Thierstein, 1971
Microstaurus chiastius (Worsley, 1971) Bralower et al., 1989
Microstaurus quadratus Black, 1971
Nannoconus erbae Casellato, 2010
Nannoconus globulus (Brönnimann, 1955) subsp. *globulus* Bralower *in* Bralower et al., 1989
Nannoconus globulus (Brönnimann, 1955) subsp. *minor* Bralower *in* Bralower et al., 1989
Nannoconus infans Bralower *in* Bralower et al., 1989
Nannoconus kamptneri (Brönnimann, 1955) subsp. *minor* Bralower *in* Bralower et al., 1989
Nannoconus puer Casellato, 2010
Nannoconus steinmannii (Kamptner, 1931) subsp. *minor* Deres & Achéritéguy, 1980
Nannoconus wintereri Bralower & Thierstein *in* Bralower et al., 1989
Polycostella beckmannii Thierstein, 1971
Polycostella senaria Thierstein, 1971
Rhagodiscus asper (Stradner, 1963) Reinhardt, 1967
Umbria granulosa subsp. *granulosa* Bralower & Thierstein *in* Bralower et al., 1989
Watznaueria barnesiae (Black *in* Black & Barnes, 1959) Perch-Nielsen, 1968
Watznaueria britannica (Stradner, 1963) Reinhardt, 1964
Watznaueria communis Reinhardt, 1964
Watznaueria fossacincta (Black, 1971a) Bown *in* Bown & Cooper, 1989
Watznaueria manivitiae (Bukry, 1973) Moshkovitz & Ehrlich, 1987
Zeugrhabdotus cooperi Bown, 1992b
Zeugrhabdotus embergeri (Noël, 1958) Perch-Nielsen, 1984
Zeugrhabdotus erectus (Deflandre *in* Deflandre & Fert, 1954) Reinhardt, 1965
Zeugrhabdotus fluxus Casellato, 2010